Mini viral RNAs act as innate immune agonists during influenza virus infection

Aartjan J.W. te Velthuis[1,2,§,*], Joshua C. Long[1,§], David L.V. Bauer[1,§], Rebecca L.Y. Fan[3], Hui-Ling Yen[3], Jane Sharps[1], Jurre Y. Siegers[4], Marian J. Killip[1,5], Hollie French[2], Maria José Oliva-Martín[1], Richard E. Randall[5], Emmie de Wit[6], Debby van Riel[4], Leo L.M. Poon[3], Ervin Fodor[1,*]

[1] Sir William Dunn School of Pathology, University of Oxford, South Parks Road, Oxford OX1 3RE, United Kingdom.

[2] Division of Virology, Department of Pathology, University of Cambridge, Addenbrooke's Hospital, Hills Road, Cambridge CB2 0QQ, United Kingdom.

[3] School of Public Health, University of Hong Kong, 21 Sassoon Road, Pokfulam, Hong Kong SAR, China.

[4] Department of Viroscience, Erasmus Medical Centre, 3015 CN, Rotterdam, The Netherlands.

[5] Biomedical Sciences Research Complex, University of St Andrews, North Haugh, St Andrews, Fife KY16 9ST, United Kingdom.

[6] Laboratory of Virology, Division of Intramural Research, National Institute of Allergy and Infectious Diseases, National Institutes of Health, Hamilton, Montana, USA

[§] These authors contributed equally to this work.

[*] Corresponding authors.

The molecular processes that determine the outcome of influenza virus infection in humans are multifactorial and involve a complex interplay between host, viral, and bacterial factors[1]. However, it is generally accepted that a strong innate immune dysregulation known as 'cytokine storm' contributes to the pathology of infections with 1918 H1N1 pandemic or highly pathogenic avian influenza viruses (HPAIV) of the H5N1 subtype[2-4]. The RNA sensor Retinoic acid-inducible gene I (RIG-I) plays an important role in sensing viral infection and initiating a signalling cascade that leads to interferon (IFN) expression[5]. Here we show that short aberrant RNAs (mini viral RNAs; mvRNAs), produced by the viral RNA polymerase during the replication of the viral RNA genome, bind and activate RIG-I, and lead to the expression of interferon-β. We find that erroneous polymerase activity, dysregulation of viral RNA replication, or the presence of avian-specific amino acids underlie mvRNA generation and cytokine expression in mammalian cells. By deep-sequencing RNA samples from lungs of ferrets infected with influenza viruses we show that mvRNAs are generated during infection in vivo. We propose that mvRNAs act as main agonists of RIG-I during influenza virus infection.

The negative sense viral RNA (vRNA) genome segments of influenza A viruses, as well as the complementary RNA (cRNA) replicative intermediates, contain 5′ triphosphates and partially complementary 5′ and 3′ termini that serve as the viral promoter for replication and transcription of the viral RNA genome[6]. RIG-I has been shown to bind and be activated by the dsRNA structure formed by the termini of influenza virus RNAs[7,8]. However, it remains unclear how RIG-I gains access to this dsRNA structure. Both vRNA and cRNA are assembled into ribonucleoprotein complexes (vRNP and cRNP, respectively) in which the viral RNA polymerase, a complex of the viral proteins PB1, PB2 and PA, associates with the partially complementary termini, while the rest of the RNA is bound by oligomeric nucleoprotein (NP)[6] (Fig. 1a). The tight binding of the 5′ and 3′ termini of vRNA and cRNA by the RNA polymerase[9] is likely to preclude an interaction with RIG-I. Moreover, it has been demonstrated that IFN expression is triggered only in a fraction of influenza virus infected cells[10,11], suggesting that influenza viruses efficiently hide their genome segments during infection by replicating them in the context of RNPs[11]. This led to the proposal that an aberrant RNA replication product might be binding to

RIG-I and triggering IFN expression[12]. The influenza virus polymerase is known to generate defective interfering (DI) RNAs, which are ≥178 nt long subgenomic RNAs generated during high multiplicity infections[13], and small viral RNAs (svRNAs), which are 22-27 nt long and correspond to the 5′ end of vRNA segments. However, svRNAs have been shown not to be involved in the induction of antiviral cellular defences[14] and DI RNAs assemble into RNP structures (Fig. 1a), as demonstrated for a 248 nt long DI RNA[15], potentially precluding their interaction with RIG-I. Therefore, it remains unclear what kind of viral RNA species is recognised by RIG-I (Fig. 1a) and why different influenza virus strains trigger dramatically different levels of IFN expression[2,3,16].

Engineered viral RNAs shorter than 149 nt but containing both the 5′ and 3′ termini of vRNAs can be transcribed and replicated by the viral polymerase in the absence of NP[17], suggesting that they do not form canonical RNP structures. We call these short viral RNAs mvRNAs (Fig. 1a). To investigate which class of viral RNA is responsible for triggering IFN expression, we expressed a full-length segment 4 vRNA (1775 nt long) or its truncated versions, a 245 nt long DI RNA and 77 nt long mvRNA, in HEK 293T cells together with viral polymerase and NP and measured the activation of the IFN-β promoter (Fig. 1b). We found that the expression of mvRNAs induced significantly higher IFN expression than full-length vRNA or DI RNA, comparable to the levels induced by transfection of 2 μg of poly(I:C), a known activator of IFN expression[18]. Similar results were obtained with segment 5 and 6 vRNAs and their truncated DI RNA and mvRNA versions (Fig. 1b). To determine the optimal mvRNA length that triggers IFN-β promoter activation, we expressed 47 to 246 nt long vRNAs derived from segment 5 together with viral polymerase and NP and measured the activity of the IFN-β promoter. We found that the replication of 56 to 125 nt long mvRNAs resulted in significantly higher IFN-β promoter activity than the replication of RNAs shorter than 56 nt or longer than 125 nt (Fig. 1c and Supplementary Fig. 1a,b).

To address whether these engineered short mvRNAs triggered IFN expression via RIG-I, we co-expressed viral RNAs with polymerase and NP in HEK 293T RIG-I knockout or control cells engineered to express luciferase in response to the activation of the IFN-β promoter. We found that 56 to 125-nt long mvRNAs induced only background levels of luciferase in RIG-I knockout cells, even though the expression

of RIG-I or transfection of poly(I:C) resulted in significant activation of the IFN-β promoter (Fig. 1d and Supplementary Fig. 1c). By contrast, significant levels of luciferase activity were detected in wildtype cells (Fig. 1d). mvRNAs of 56 to 125 nt induced the strongest activation of the IFN-β promoter, in agreement with the data above (Fig. 1c,d and Supplementary Fig. 1c,d). To address whether mvRNAs trigger the activation of IFN-β expression through binding to RIG-I, we immunoprecipitated myc-RIG-I from cells expressing RNAs of 47 to 583 nt. We observed that mvRNAs of 56 to 125 nt were specifically enriched in RIG-I immunoprecipitates (Fig. 1e and Supplementary Fig. 1e). No mvRNAs were detected in the myc-EGF negative control immunoprecipitates (Fig. 1e). To test if mvRNAs also activate RIG-I, we incubated purified myc-RIG-I with an *in vitro* transcribed 76 nt mvRNA and measured $^{32}P_i$ release. We found that a triphosphorylated 76 nt mvRNA induced higher levels of ATPase activity than a dephosphorylated 76 nt mvRNA, while no ATPase activity was observed when we incubated a RIG-I mutant with the triphosphorylated 76 nt mvRNA (Supplementary Fig. 1f,g). Overall, these results demonstrate that mvRNAs longer than 47 and shorter than 125 nt are bound by RIG-I, which results in RIG-I activation and the induction of IFN-β expression. This is in agreement with findings that reconstitution of full-length influenza virus vRNPs leads to only low levels of IFN expression unless the cells are pre-treated with IFN[19] and the hypothesis that aberrant replication products trigger the IFN induction cascade[12].

We next asked whether mvRNAs are made during influenza virus infection. We infected HEK 293T cells with influenza A/WSN/33 (H1N1) (abbreviated as WSN) and analysed viral RNAs by RT-PCR of segment 1, RT-PCR of all segments using universal primers, or deep-sequencing of the total small RNA fraction (RNAs 17 to 200 nt in length) (Supplementary Fig. 2a,b). We found only very low levels of mvRNAs and, consistently, observed no significant IFN expression (Fig. 2a,b). We hypothesised that mvRNAs are only generated as a consequence of dysregulated viral RNA replication. To test this, we overexpressed viral RNA polymerase prior to infection to generate an imbalance between polymerase and NP levels, which is known to induce innate immune signalling[20]. Under this condition we found significantly higher levels of mvRNAs and IFN expression, while simultaneous overexpression of NP and polymerase reduced mvRNA and IFN production (Fig. 2a). We verified the identity of mvRNAs using gel isolation and Sanger sequencing

(Supplementary Fig. 2c) as well as deep sequencing (Fig. 2b). We found that the majority of mvRNAs were derived from the PB1-, HA-, NP- and NA-encoding vRNA segments (Fig. 2c) and that mvRNAs had a size distribution with a peak around 55 to 64 nt (Fig. 2d and Supplementary Fig. 2d). In addition to mvRNAs, we also identified complementary mini viral RNAs (mcRNAs).

Analysis of mvRNA sequences suggests that mvRNAs are generated via an intramolecular copy-choice mechanism that tolerates 3' mismatches or skipped bases (Fig. 2e,f). The generation of mvRNAs can be explained by the separation of the template and nascent product RNAs by backtracking[21], followed by template translocation until base pairing between template and nascent product RNA is re-established (Fig. 2f,g). This process may be induced by an imbalance between viral polymerase and NP levels (Fig. 2a and Supplementary Fig. 3a).

In humans, infection with the 1918 H1N1 pandemic virus or H5N1 HPAIV lead to strong innate immune activation[2,3,16]. To address whether mvRNAs could contribute to this phenomenon, we investigated the replication of a 246 nt RNA by the polymerase of these viruses. We found that the polymerases of the highly virulent A/Brevig Mission/1/18 (H1N1) (abbreviated as BM18) pandemic virus and the A/duck/Fujian/01/02 (H5N1) (abbreviated as FJ02) HPAIV generated higher levels of mvRNAs than the polymerases of WSN and A/Northern Territory/60/68 (H3N2) (abbreviated as NT60) viruses, even in the presence of high NP concentrations (Fig. 3a). No mvRNAs were observed in a control with an inactive WSN polymerase that had two point mutations in the polymerase active site (PB1a). We confirmed that the mvRNAs produced by the BM18 polymerase were similar to the WSN mvRNAs (Supplementary Fig. 3b). Isolation of total RNA from cells expressing polymerase of the BM18 or FJ02 virus and its subsequent transfection into HEK 293T cells resulted in significantly higher IFN-β promoter activity compared to when RNA from cells expressing WSN, NT60, or active site mutant WSN PB1a polymerase was transfected (Fig. 3a).

The identification of mismatches during the generation of mvRNAs (see Fig. 2e) suggests that mvRNA production might be dependent on polymerase fidelity. To investigate this further, we introduced a V43I mutation, which has been shown to confer high-fidelity on an H5N1 influenza virus polymerase[22], into the PB1 subunit of the BM18 polymerase ($BM18^{hf}$). We found that mvRNA levels were significantly

reduced in the presence of BM18^{hf}, with a corresponding reduction in IFN-β promoter activity (Fig. 3a). Together, the observations in Fig. 2a, Fig. 3, and Supplementary Fig. 3a suggest that dysregulation of viral RNA replication, e.g. by limiting NP availability, and replication by HPAIV polymerases in mammalian cells generates mvRNAs by employing an error-prone copy-choice mechanism, such as proposed for recombination in positive-strand RNA viruses[23].

We next asked whether a particular BM18 polymerase subunit is the determinant of mvRNA production and replaced individual polymerase subunits of the BM18 polymerase with subunits of the WSN polymerase in the 246 nt RNA replication assay. We found that particularly replacement of the BM18 PB2 subunit with the WSN PB2 subunit eliminated the generation of mvRNAs (Supplementary Fig. 4a). Interestingly, the BM18 influenza PB2 subunit has been linked to the enhancement of both the kinetics and the magnitude of the host response to viral infection, leading to the induction of strong inflammatory responses in the lungs of infected mice[24]. To identify PB2 amino acids involved in mvRNA formation, we aligned the BM18, WSN, NT60 and FJ02 PB2 sequences and found four amino acids that distinguish the BM18 and FJ02 polymerases from the WSN and NT60 polymerases: 9 (D→N), 64 (M→T), 81 (T→M), and 661 (A→T) (Supplementary Fig. 4a). Each of these amino acids has been implicated in avian to mammalian host adaptation[25] and, interestingly, all three N-terminal PB2 adaptive amino acids map to the template exit channel of the RNA polymerase (Fig. 3b)[6]. We generated single mutations N9D, T64M, M81T, and double mutations N9D+T64M and N9D+M81T in the PB2 subunit of the WSN polymerase and found that mutants N9D and M81T and the double mutants N9D+T64M and N9D+M81T significantly increased mvRNA formation (Fig. 3c) and IFN-β promoter activity (Fig. 3c,d). However, the levels of mvRNAs generated by these mutants did not reach the levels generated by the BM18 polymerase indicating that further amino acids contribute to mvRNA production. In line with our observations, WSN viruses that contain a PB2 N9D substitution or other PB2 mutations near the template exit channel have been reported to induce higher IFN-β expression than wild-type WSN[26,27].

To address whether mvRNAs form during infection of mammalian cells, we infected A549 cells with WSN, the highly pathogenic avian strain A/Vietnam/1203/04 (H5N1) (abbreviated as VN04), and the VN04 virus with the PB1 V43I high-fidelity

mutation (abbreviated as VN04^{hf}). Infections with VN04 resulted in high levels of mvRNAs, while WSN infections produced only very low levels (Fig. 4a). Infections with VN04^{hf} resulted in significantly reduced mvRNA levels compared to the wild-type VN04 virus. These results demonstrate that mvRNAs are formed during influenza virus infection of lung epithelial cells and that polymerase fidelity is an important determinant of mvRNA formation (Fig. 4a).

To investigate whether there is a link between mvRNA production and virus-induced innate immune responses we performed RNAseq of cells infected with VN04 and VN04^{hf} viruses and examined which genes were differentially expressed in response to mvRNA levels. Despite significantly different mvRNA levels produced by VN04 and VN04^{hf}, viral mRNA levels were similar (Supplementary Data 1), in agreement with previous findings that the V43I mutation has only a marginal effect on virus replication[22]. Gene Ontology (GO) analysis (Fig. 4b) showed that basic cellular functions were significantly compromised in VN04 infection relative to VN04^{hf}, consistent with a greater level of cell death, which is known to exacerbate inflammation[28]. In addition, we observed that genes associated with innate immune responses showed a significant increase in expression in response to higher mvRNA levels (Fig. 4b). Overall, these observations are indicative of a link between erroneous polymerase activity, mvRNA synthesis, and innate immune activation and the induction of cell death. Furthermore, as VN04 exhibited a 10-fold higher lethality compared to V04^{hf} in mice[22], our data also suggest a link between mvRNA levels and virulence.

To address whether mvRNAs are produced in infection of animal models, we analysed RNA samples from ferret lungs one and three days after infection with highly pathogenic avian A/Indonesia/5/2005 (H5N1) (abbreviated as IN05), 2009 swine-origin pandemic A/Netherlands/602/2009 (H1N1) (abbreviated as NL09) or the BM18 pandemic virus[29,30]. mvRNAs were present in all infected lung samples one day after infection, with mvRNA levels particularly high in the BM18 infected ferret lungs (Fig. 4c, Supplementary Fig. 5). GO analysis on the ferret lung samples taken one and three days post infection, showed an up-regulation of apoptosis and innate immune responses as function of mvRNA level, independently of viral titre or the day post infection (Fig. 4d).

In summary, we identify mvRNAs, a class of influenza virus RNAs, that act as the main agonists of the pathogen recognition receptor RIG-I during influenza virus

infection (Fig. 4e). mvRNAs are produced as a result of aberrant replication of the viral RNA genome by the viral RNA polymerase. Polymerase fidelity and host-specific amino acids are determinants of the ability of the viral polymerase to produce mvRNAs, which are distinct from DI RNAs and full length viral RNA segments in that they can be efficiently replicated in the absence of NP and do not form canonical RNPs[17]. These features of mvRNAs are likely to be critical for their preferential recognition by RIG-I over DI RNAs and full-length RNA segments. We further demonstrate that mvRNA production is linked to increased cytokine expression and cell death. Our observations thus strongly suggest that mvRNAs are a contributing factor to influenza virus virulence. We speculate that production of high levels of mvRNAs by the polymerases of the 1918 pandemic and highly pathogenic avian influenza viruses and the resulting increased innate immune activation contribute to the cytokine storm phenomenon underlying the high virulence of these viral strains. The effects of mvRNAs are likely modulated by viral factors, such as the immunomodulatory NS1 and PB1-F2 proteins[12] (Fig. 4e). Further studies are required to assess mvRNA levels generated by various influenza virus strains, including seasonal strains, and their effect on virulence.

Methods

Ethics and biosafety

All work with highly pathogenic H5N1 viruses in A549 cells was conducted in the Biosafety Level-3 laboratory at the LKS Faculty of Medicine, The University of Hong Kong, under guidelines and ethics approved by the Committee on the Use of Live Animals in Teaching and Research (CULATR). Ferret experiments with IN05 and NL09 were described previously[29] and conducted in the Biosafety Level-3 laboratory of the Erasmus Medical Centre in compliance with European guidelines (EU directive on animal testing 86/609/EEC) and Dutch legislation (Experiments on Animals Act, 1997), after approval by the independent animal experimentation ethical review committee of the Netherlands Vaccine Institute (permit number 200900201). Ferret experiments with BM18 were described previously[30] and approved by Institutional Animal Care and Use Committee of Rocky Mountain Laboratories, National Institutes of Health, and conducted in an Association for Assessment and Accreditation of

Laboratory Animal Care international-accredited facility according to the guidelines and basic principles in the United States Public Health Service Policy on Humane Care and Use of Laboratory Animals, and the Guide for the Care and Use of Laboratory Animals. Sample inactivation and shipment was performed according to standard operating procedures for the removal of specimens from high containment and approved by the Institutional Biosafety Committee.

Plasmids

Plasmids expressing the three polymerase subunits and NP of influenza A/WSN/33 (H1N1)[31], A/Northern Territory/60/68 (H3N2)[32], A/duck/Fujian/01/02 (H5N1)[32] (all pcDNA3-based), and A/Brevig Mission/1/18 (H1N1)[33] (pCAGGS-based) have been described. A PB2 E627K mutation was introduced into the A/duck/Fujian/01/02 (H5N1) PB2 subunit to enable the FJ02 polymerase to efficiently replicate vRNA in mammalian cells. Plasmids expressing mutant PB1a (D445A/D446A)[34], and mutant PB2 (N9D)[26], of influenza A/WSN/33 (H1N1) virus have been described previously. Full-length or internally truncated vRNAs were expressed from plasmids under the control of cellular RNA polymerase I promoter[35]. Luciferase reporter plasmid under the control of the IFN-β promoter (pIFΔ(-116)lucter), the β-galactosidase reporter plasmid (pJatLacZ) under the control of a constitutive promoter (β-gal), pcDNA-Myc-RIG-I expressing myc-tagged RIG-I, and pcDNA-myc-proEGF have been described previously[36,37]. To construct plasmids expressing mutant PB1, PB2 proteins and myc-RIG-I (myc-RIG-I mut; which contains the mutations K851A, K858A and K861A), the plasmids expressing wild-type proteins were subjected to site-directed mutagenesis using the primers listed in Supplementary Table 1.

Cells and antibodies

Human embryonic kidney HEK 293T cells were originally sourced from the ATCC, stored in the Dunn School cell bank at the University of Oxford, and mycoplasma tested, but not authenticated prior to our experiments. A549 cells were originally sourced from the ATCC and cultured at the University of Hong Kong. Cells were cultured in DMEM (Sigma-Aldrich) and 10% FCS. Western blots were performed using NP antibody GTX125989 (GeneTex), Myc antibody GTX115046 (GeneTex), RIG-I antibody GTX85488 (GeneTex), and PB2 antibody GTX125926 (GeneTex).

Wild-type and RIG-I knockout HEK 293T cells expressing luciferase in response to the activation of the IFN-β promoter were described previously[38].

Statistical testing

In all figures, error bars indicate standard deviation with sample sizes as indicated in figures or figure legends. Evaluation of the statistical significance between group means was performed across all experiments according to the following criteria: (i) in the case where a comparison of a single variable was made between only two groups, an unpaired t-test was used; (ii) in the case of comparisons between three of more groups of measurements derived from a single independent variable (e.g. IFN-β induction as a function of RNA length), one-way ANOVA was used and P-values were corrected for multiple comparisons using either Dunnett's test (when a single group was taken as a reference/control to which all other groups were compared) or the Bonferroni method (when specific pairs of groups were compared to one another); (iii) in the case of comparisons between three of more groups of measurements derived from two independent variables (e.g. IFN-β induction as a function of RNA length and RIG-I expression), two-way ANOVA was used and P-values were corrected for multiple testing using the Bonferroni method; (iv) in the case of comparisons between three of more groups of log-distributed data (e.g. viral titres), measured values were first $\log_{10}$ transformed and then compared using one-way ANOVA, with P-values corrected for multiple comparisons by controlling the false discovery rate (FDR) to be <0.05 using the two-stage step-up method of Benjamini, Kreiger, and Yekutieli. For the evaluation of the statistical significance of the relationship between two measured values (e.g. fold increase in IFN-β induction *vs.* mvRNA level), linear regression analysis was used, with the P-value indicating the probability of the null hypothesis (no linear relationship), and the goodness of fit reported as r^2. Statistical testing related to differential gene expression analysis is detailed below, and was performed in R; all other statistical tests were performed using GraphPad Prism.

RNP reconstitution assays and quantitative RNA analysis

RNP reconstitution assays were carried out in 24-well plates out as described previously[34,39]. Briefly, 0.25 μg of the plasmids pcDNA3-NP, pcDNA3-PB2,

pcDNA3-PB1, pcDNA3-PA, and a pPOLI plasmid encoding full-length or truncated vRNA templates (for list of vRNA templates used see Supplementary Table 2) were transfected into HEK 293T cells using Lipofectamine 2000 (Invitrogen) according to the manufacturer's instructions. Twenty-four hours post transfection, RNA was extracted using TRI Reagent (Sigma-Aldrich) and dissolved in RNase free water. For quantitative primer extensions, reverse transcription was carried out using SuperScript III reverse transcriptase (Thermo Fisher Scientific) with ^{32}P-labelled oligonucleotides complementary to vRNA-derived RNA species and ribosomal 5S rRNA (for primers see Supplementary Table 3). cDNA synthesis was stopped with 10 µl loading dye (90% formamide, 10 mM EDTA, xylene cyanole, bromophenol blue) and ^{32}P-labelled cDNAs generated with primer NP- were resolved by 12% denaturing PAGE (19:1 acrylamide/bis-acrylamide, 1x TBE buffer, 7 M urea). ^{32}P-labelled cDNAs generated with primer NP-2 were resolved by 20% denaturing PAGE. The radiolabelled signals were imaged using phosphorimaging on a FLA-5000 scanner (Fuji), and analysed using AIDA (RayTek) and Prism 7 (GraphPad). In all experiments, the apparent RNA levels were background corrected using the PB1 active site mutant (PB1a) signal and normalised to the 5S rRNA control. Statistical analysis of data from at least three independent experiments was carried out using ANOVA.

RNP reconstitution assays and qualitative RNA analysis

For segment-specific qualitative RNA analysis by RT-PCR, RNA was treated with DNase (Promega) for 10 min according to the manufacturer's instructions and reverse transcribed using SuperScript III and the PB2 primers listed in Supplementary Table 3. cDNA was amplified using Q5 polymerase (NEB) and the primers listed in Supplementary Table 3. PCR products were analysed on 1.5% agarose gels in 0.5x Tris-acetate-EDTA (TAE) buffer. For qualitative RT-PCR using universal primers, DNase treated RNA was reverse transcribed using the Lv3aa and Lv3ga primers listed in Supplementary Table 3 and Superscript III at 37 ºC for 30 min. Second strands synthesis was performed with primer Lv5 and Q5 polymerase (NEB) at 47 ºC for 10 min, followed by a further extension at 72 ºC for 3 min. The primer excess in the reactions was removed by incubating the second strand reaction with 1 U of exonuclease VII (NEB) at 37 degrees Celsius for 1 h. Following inactivation of the exonuclease at 95 ºC for 10 min, the DNA was amplified using Q5 polymerase, and primers P5 and i7 for 25 cycles. PCR products were analysed by 6% PAGE.

Luciferase-based interferon expression assays

For luciferase assays, RNP reconstitutions were performed in wild-type HEK 293T cells or HEK 293T cells engineered to express luciferase from the IFN-β promoter. RNP reconstitutions were performed in a 24-well format by transfecting 0.25 μg of the plasmids pcDNA3-NP, pcDNA3-PB2, pcDNA3-PB1, pcDNA3-PA, a pPOLI plasmid encoding full-length or truncated vRNA templates using lipofectamine2000 (Invitrogen). For RNP reconstitutions in wild-type HEK 293T cells, 100 ng of pIFΔ(-116)lucter and pJatLacZ were co-transfected with the polymerase expressing plasmids. Twenty-four hours post transfection, cells were harvested in PBS and resuspended in Reporter Lysis buffer (Promega). Luciferase activity was measured using a Luciferase Assay System (Promega) and a GloMax (Promega), and normalised using the β-galactosidase signal measured using ortho-Nitrophenyl-β-galactoside (ONPG) and a GloMax. The background was subtracted using signals obtained from cells transfected with an empty pcDNA3. Luciferase levels were corrected for viral RNA levels obtained with primer extensions and a ^{32}P-labelled NP-2 primer (Supplementary Table 3). For total RNA transfections, 100 ng of total RNA was transfected with 100 ng of pIFΔ(-116)lucter and pJatLacZ using Lipofectamine2000. Analysis of luciferase expression was performed as described above. Statistical analysis was carried out using ANOVA.

Immunoprecipitations

For myc-RIG-I immunoprecipitations, 10 cm dishes with HEK 293T cell were transfected with 3 μg pcDNA3-NP, pcDNA3-PB2, pcDNA3-PB1, pcDNA3-PA, pcDNA-myc-RIG-I or pcDNA-myc-EGF, and a pPOLI plasmid encoding either a full-length or truncated vRNA template using Lipofectamine 2000. Twenty-four hours post transfection, the cells were harvested in cold PBS and lysed in 600 μl Tris lysis buffer (50 mM Tris-HCl, pH 8.0; 5% glycerol; 0.5% Igepal; 200 mM NaCl; 1 mM EDTA; 1 mM DTT; and 1x EDTA-free protease inhibitor (Roche)) on ice for 1 h. The lysates were cleared at 10,000 *g* for 5 min. Six μg of anti-myc antibody (Sigma-Aldrich) was added to 0.5 ml of cleared lysate and mixed at 4 ºC for 1.5 h. The lystate-antibody mix was bound to Dynabeads (Novex) at 4 ºC for 1.5 h, washed 3 times with IgG wash buffer (10 mM Tris-HCl pH 8.0; 150 mM NaCl; 0.1% Igepal; 1

mM PMSF; 1 mM EDTA), and finally analysed for bound RNA and protein. Statistical analysis of data from three independent experiments was carried out using ANOVA.

ATPase assay

For wild-type and mutant myc-RIG-I purification, HEK 293T cell were transfected with 5 μg pcDNA-myc-RIG-I or pcRNA-myc-RIG-I mut using Lipofectamine 2000. Twenty-four hours post transfection, the cells were harvested in cold PBS and lysed in lysis buffer (50 mM Hepes, pH 8.0; 5% glycerol; 0.5% Igepal; 200 mM NaCl; 2 mM $MgCl_2$; 10 mM $CaCl_2$; 1 mM DTT; 1 U/ml Micrococcal Nuclease (Thermo Scientific); and 1x EDTA-free protease inhibitor) on ice for 1 h. Three μg of anti-myc antibody was next added per 0.5 ml of cleared lysate and mixed at 4 ºC for 1.5 h. The lystate-antibody mix was bound to Protein G Mag Sepharose Xtra beads (GE Healthcare) at 4 ºC for 1.5 h, washed 6 times with 20 column volumes of RIG-I wash buffer (50 mM Hepes, pH 8.0; 200 mM NaCl; 0.1% Igepal; 5% glycerol; 1 mM PMSF; 2 mM $MgCl_2$) at 4 ºC for 10 min, and finally myc-RIG-I was eluted from beads in 1 column volume wash buffer containing 0.5 mg/ml c-myc peptide (Pierce) for 15 min at 4 ºC. Activity assays were performed in 50 mM Hepes pH 8.0, 150 mM NaCl, 2 mM $MgCl_2$, 5 mM DTT, and 0.1 μM [γ-^{32}P]ATP. [γ-^{32}P]ATP and $^{32}P_i$ were resolved using PEI-cellulose TLC plates (Sigma-Aldrich) in 0.4 M KH_2PO_4 pH 3.4.

Cell and animal infections

HEK 293T cells were infected with influenza A/WSN/33 (H1N1) virus, free of DI RNAs, at a multiplicity of infection (MOI) of 5. RNA was extracted 5 h post infection and analysed using deep sequencing or qualitative RT-PCR. 6-wells containing A549 cells were infected with A/WSN/33 (H1N1), A/Vietnam/1203/04 (H5N1), or A/Vietnam/1203/04 (H5N1) with the V43I mutation with an MOI of 5. RNA was extracted 8 hours post infection and analysed using deep sequencing or qualitative RT-PCR. Ferret (*Mustela putorius furo*) lung tissue was obtained from male ferrets infected with A/Indonesia/5/2005 (H5N1) or A/Netherlands/602/2009 (H1N1)[29], or female ferrets infected with A/Brevig Mission/1/1918 (H1N1)[30]. Ferrets were randomly assigned to groups of four before inoculation. A single ferret (lung titre = 7.6×10^1 $\log_{10}TCID_{50}$/g) was excluded from analysis on the basis of its apparent lack

of infection. Ferret RNA was isolated from lung tissue samples using Trizol (Invitrogen) and analysed using qualitative RT-PCRs and next generation mvRNA sequencing with universal primers and quantitative mRNA sequencing.

Sequence alignment and structural modelling

PB2 amino acid sequences from influenza A viruses A/WSN/33 (H1N1), A/Brevig Mission/1/18 (H1N1), A/Northern Territory/60/68 (H3N2), and A/duck/Fujian/01/02 (H5N1) were aligned using Muscle 3.0 and visualised using ESPript[40]. The bat influenza A virus polymerase structure (PDB 4WSB) was visualised in Pymol 1.6.

Next generation sequencing of mvRNAs using adapters

Total cell RNA from transfected or infected cells was isolated using Tri Reagent (Sigma) or Trizol (Invitrogen) according to the manufacturer's instructions and fractionated into small (17-200 nt) and large (>200 nt) RNA fractions using an RNA Clean and Concentrator kit (Zymo Research). Next, the small RNA fraction was denatured at 70 ºC for 2 min and subsequently treated with 2 U of XRN-1 in NEB buffer 2 at 37 ºC for 15 min to deplete miRNAs. Next, XRN-1 was inactivated by adding 10 mM EDTA and incubating the reaction at 70 ºC for 10 min. Viral triphosphorylated RNAs were converted to monophosphorylated RNAs by adding 5 U of RNA 5' Pyrophosphohydrolase (RppH) and 10 mM $MgCl_2$ and incubating the reactions at 37 ºC for 15 min. RNA was purified using an RNA Clean and Concentrator kit and libraries for deep sequencing were prepared using the NEBNext Small RNA Library Prep Kit according to the manufacturer's instructions. To ensure accurate quantitation after PCR amplification, the concentration of each library was measured by qPCR on a StepOnePlus instrument (ABI) and the number of PCR cycles used to subsequently amplify the remaining library material was calibrated so as to ensure the PCR was in the early stage of exponential amplification and to not over-cycle the PCR reactions. Amplified sequencing libraries were purified on a 6% Novex TBE PAGE according to the manufacturer's instructions to remove primer-dimers. Paired-end sequencing (2x75bp) on an Illumina HiSeq 4000 was carried out by the Oxford Genomics Centre, Wellcome Trust Centre for Human Genetics (Oxford, UK). It is important to note that the existence of mvRNAs has likely been overlooked till now, because i) RNA isolation protocols vary in their capacity to recover small RNAs, ii) RT-PCR products from mvRNAs form a diffuse fast-migrating band on

standard agarose gels that may be mistaken for primer-dimers, iii) conventional RNA deep sequencing protocols discard short library fragments, and iv) standard ligation-based deep sequencing protocols do not detect viral transcripts with a 5′-triphosphate group.

Next generation sequencing of mvRNAs using universal primers

To spike viral RNA for quantitative sequencing, 0.2 µl of 100 pM spike RNA (Supplementary Table 2) was added to 40 ng of the small RNA fraction (see above). The RNA mixture was next converted into cDNA using primers Lv3aa, Lv3ga and Lc3 and Superscript III (Invitrogen) at 37 ºC for 30 min. Second strand synthesis was performed using Q5 polymerase (NEB) and primers Lv5, Lc3a, and Lc3g at 47 ºC for 10 min, followed by a further extension at 72 ºC for 3 min. The excess of barcoded primers was removed by incubating the second strand reaction with 1 U of exonuclease VII (NEB) at 37 ºC for 1 h. The exonuclease was inactivated at 95 ºC for 10 min. Next, the DNA was amplified using Q5 polymerase, primer P5 and i7 index primers (Lexogen), and subsequently sequenced on a NextSeq 500 sequencer (Illumina).

Preparation of reference genome files for deep sequencing of mvRNAs

Prior to mapping, a reference genome file was prepared from relevant viral reference sequences in Genbank (see above). For the analysis of sequencing libraries prepared using universal influenza virus primers, the 5′ and 3′ viral promoter sequences of each segment were modified to match the degenerate universal primer sequences used in sample preparation (see Supplementary Table 3), and the sequences of the spiked-in mvRNA quantitation standards (see Supplementary Table 2) were appended to the reference genome. For WSN, VN04, and VN04^{hf} viruses, deep-sequencing data of mRNA generated in A549 cell infections (above) was exploited to generate updated reference genome files: the *mpileup* and *consensus* commands in the *bcftools* software package[41] were used following mapping of non-host mRNA reads to the relevant viral reference genome using *STAR* aligner[42].

Data processing pipeline for deep sequencing of mvRNAs using universal influenza virus primers

Raw sequencing reads were first trimmed to remove sequencing adaptor sequences and reads with quality scores less than 20 using the *cutadapt* software package[43] and the 8-nt unique molecular identifier (UMI) at the start of each read were removed from the sequence and appended to the read ID line of the FASTQ file using the *extract* command from the *umi_tools* software package[44]. Sequencing reads were then mapped end-to-end to the appropriate viral reference genome using the *STAR* aligner[42], and permitting sequencing reads to have long internal deletions (i.e. an mvRNA, interpreted as splicing by STAR) with at least 16 nt anchored on either side of the deletion (*--outSJfilterOverhangMin 16 16 16 16*). The default settings of *STAR* were modified so that no alignment scoring penalty was given for an internal deletion and no preference was given to internal deletions that overlapped particular sequence motifs (*--scoreGapNoncan 0 --scoreGapGCAG 0 --scoreGapATAC 0*), and to ensure accurate quantitation, only the top-scoring alignment was included in the outputted BAM file (*--outSAMmultNmax 1*), which was sorted and indexed using *samtools*[45]. An aligned read was counted as an mvRNAs if it was anchored to the viral reference genome at the 5′ end in vRNA sense and contained an internal deletion (called as a splice junction by *STAR*), and the total numbers of mvRNAs and spiked-in quantitation standards were tallied using the *idxstats* command of *samtools*. mvRNA levels relative to the quantitation were then reported as number of reads per million mapped (RPM) quantitation standard. To validate the qPCR protocol used to prevent over-cycling of sequencing libraries, the quantitation was then repeated following removal of PCR duplicates, exploiting the UMI appended to each read, using the *umi_tools dedup* command, and counting the various mvRNA species as unique using the *--spliced-is-unique* option. The identities of the individual mvRNAs were then extracted from the *SJ.out.tab* file generated by STAR.

Data processing pipeline for deep sequencing of mvRNAs using adapter ligation

Raw sequencing reads were first trimmed using the *cutadapt* software package[43] to remove RNA adapters, sequencing adapters, and reads with quality scores less than 20. Since adapter ligation captures both host-derived and virus-derived small RNA species, reads were first mapped end-to-end to the DASHR database of human small RNAs[46] using the *STAR* aligner[42], with spliced alignments disabled (*--alignIntronMax 1*). Non-human reads were outputted using the *--outReadsUnmapped Fastx* option, were then mapped to the appropriate viral reference genome to find mvRNAs as

described above, and quantitated relative to the total number of viral reads (RPM viral) or host reads (RPM host).

Quantitative mRNA sequencing and differential gene expression analysis

Libraries for gene expression analysis were prepared using a QuantSeq 3' mRNA-Seq Library Prep Kit FWD for Illumina (Lexogen) according to the manufacturer's instructions and sequenced on a NextSeq 500 sequencer. mRNA reads were aligned to the reference genome (CRCh38, GRCm38, or MusPutFur1.0) using the STAR read aligner[42], exploiting the built-in trimming functions to remove the first 12 bases corresponding the Lexogen random primer (*--clip5pNbases 12*) and any contaminating poly(A) tails in the sequencing reads (*--clip3pAdapterSeq AAAAAAAAAAAAAAAAAA*), as well as requiring a minimum match to the reference genome of 40 bp (*--outFilterMatchNmin 40*). Gene counts were generated using reference genome annotations (Gencode v26 for CRCh38, and Ensembl 90 for MusPutFur1.0) using the STAR command *--quantMode GeneCounts*. Differential gene expression analysis was then carried out using the DEseq2 package in R[47] to identify genes that were up- or down-regulated as a function of mvRNA levels, independently of viral load or titre. Specifically, the likelihood ratio test (LRT) was used to compare a full model (in which gene expression varies as a function of both viral load or titre, and mvRNA levels) to a reduced model (in which changes in gene expression are fully explained by viral load or titre alone) using analysis of deviance (ANODEV) to generate a P-value for the log-fold-change of each gene, which were adjusted for multiple testing by controlling the false discovery rate (FDR) using Independent Hypothesis Testing[48] and reported as q-values. mvRNA levels were determined by deep sequencing using universal influenza virus primers, as detailed above. Viral load or titre was determined by segment 6 qRT-PCR or by using previously published values[29,30]. Subsequent enrichment analysis of Gene Ontology terms specifically affected by mvRNA levels was carried out using Parametric Analysis of Gene Set Enrichment[49] via the GAGE package in R, with data from the above genome annotations, accessed via the biomaRt package[50]. Significance of enrichment for GO terms was calculated using a one-sample z-test[49] in GAGE, and P-values were adjusted for multiple testing using the Benjamini-Hochberg method and were reported as q-values.

References

1. Kash, J. C. & Taubenberger, J. K. The Role of Viral, Host, and Secondary Bacterial Factors in Influenza Pathogenesis. *The American Journal of Pathology* **185,** 1528–1536 (2015).
2. Kash, J. C. *et al.* Genomic analysis of increased host immune and cell death responses induced by 1918 influenza virus. *Nature* **76,** 105–4 (2006).
3. Kobasa, D. *et al.* Aberrant innate immune response in lethal infection of macaques with the 1918 influenza virus. *Nature* **445,** 319–323 (2007).
4. de Jong, M. D. *et al.* Fatal outcome of human influenza A (H5N1) is associated with high viral load and hypercytokinemia. *Nat. Med.* **12,** 1203–1207 (2006).
5. Pichlmair, A. *et al.* RIG-I-mediated antiviral responses to single-stranded RNA bearing 5'-phosphates. *Science* **314,** 997–1001 (2006).
6. Velthuis, te, A. J. W. & Fodor, E. Influenza virus RNA polymerase: insights into the mechanisms of viral RNA synthesis. *Nat Rev Microbiol* **14,** 479–493 (2016).
7. Kowalinski, E. *et al.* Structural basis for the activation of innate immune pattern-recognition receptor RIG-I by viral RNA. *Cell* **147,** 423–435 (2011).
8. Lee, M.-K. *et al.* Structural features of influenza A virus panhandle RNA enabling the activation of RIG-I independently of 5'-triphosphate. *Nucleic Acids Res* **44,** 8407–8416 (2016).
9. Robb, N. C. *et al.* Single-molecule FRET reveals the pre-initiation and initiation conformations of influenza virus promoter RNA. *Nucleic Acids Res* **44,** 10304–10315 (2016).
10. Russell, A. B., Trapnell, C. & Bloom, J. D. Extreme heterogeneity of influenza virus infection in single cells. *eLife* pii: e32303 (2017). doi:10.1101/193995
11. Killip, M. J., Jackson, D., Pérez-Cidoncha, M., Fodor, E. & Randall, R. E. Single-cell studies of IFN-β promoter activation by wild-type and NS1-defective influenza A viruses. *J. Gen. Virol.* **98,** 357–363 (2017).
12. Killip, M. J., Fodor, E. & Randall, R. E. Influenza virus activation of the interferon system. *Virus Research* **209,** 11–22 (2015).
13. Jennings, P. A., Finch, J. T., Winter, G. & Robertson, J. S. Does the higher order structure of the influenza virus ribonucleoprotein guide sequence rearrangements in influenza viral RNA? *Cell* **34,** 619–627 (1983).
14. Perez, J. T. *et al.* Influenza A virus-generated small RNAs regulate the switch from transcription to replication. *Proc. Natl. Acad. Sci. U.S.A.* **107,** 11525–11530 (2010).
15. Coloma, R. *et al.* The Structure of a Biologically Active Influenza Virus Ribonucleoprotein Complex. *PLoS Pathog* **5,** e1000491–10 (2009).
16. Li, H. *et al.* Internal genes of a highly pathogenic H5N1 influenza virus determine high viral replication in myeloid cells and severe outcome of infection in mice. *PLoS Pathog* **14,** e1006821 (2018).
17. Turrell, L., Lyall, J. W., Tiley, L. S., Fodor, E. & Vreede, F. T. The role and assembly mechanism of nucleoprotein in influenza A virus ribonucleoprotein complexes. *Nature Communications* **4,** 1591 (2013).
18. Kato, H. *et al.* Differential roles of MDA5 and RIG-I helicases in the recognition of RNA viruses. *Nature* **441,** 101–105 (2006).
19. Rehwinkel, J. *et al.* RIG-I Detects Viral Genomic RNA during Negative-Strand RNA Virus Infection. *Cell* **140,** 397–408 (2010).

20. Killip, M. J., Smith, M., Jackson, D. & Randall, R. E. Activation of the Interferon Induction Cascade by Influenza A Viruses Requires Viral RNA Synthesis and Nuclear Export. *J. Virol.* **88,** 3942–3952 (2014).
21. Dulin, D. *et al.* Backtracking behavior in viral RNA-dependent RNA polymerase provides the basis for a second initiation site. *Nucleic Acids Res* **43,** 10421–10429 (2015).
22. Cheung, P. P. H. *et al.* Generation and characterization of influenza A viruses with altered polymerase fidelity. *Nature Communications* **5,** 1–13 (2014).
23. Woodman, A., Arnold, J. J., Cameron, C. E. & Evans, D. J. Biochemical and genetic analysis of the role of the viral polymerase in enterovirus recombination. *Nucleic Acids Res* **44,** 6883–6895 (2016).
24. Forero, A. *et al.* The 1918 Influenza Virus PB2 Protein Enhances Virulence through the Disruption of Inflammatory and Wnt-Mediated Signaling in Mice. *J. Virol.* **90,** 2240–2253 (2016).
25. Miotto, O., Heiny, A. T., Tan, T., August, J. T. & Brusic, V. Identification of human-to-human transmissibility factors in PB2 proteins of influenza A by large-scale mutual information analysis. *BMC Bioinformatics* **9,** S18–18 (2008).
26. Graef, K. M. *et al.* The PB2 Subunit of the Influenza Virus RNA Polymerase Affects Virulence by Interacting with the Mitochondrial Antiviral Signaling Protein and Inhibiting Expression of Beta Interferon. *J. Virol.* **84,** 8433–8445 (2010).
27. Du, Y. *et al.* Genome-wide identification of interferon-sensitive mutations enables influenza vaccine design. *Science* **359,** 290–296 (2018).
28. Chan, F. K.-M., Luz, N. F. & Moriwaki, K. Programmed necrosis in the cross talk of cell death and inflammation. *Annu. Rev. Immunol.* **33,** 79–106 (2015).
29. van den Brand, J. M. A. *et al.* Comparison of Temporal and Spatial Dynamics of Seasonal H3N2, Pandemic H1N1 and Highly Pathogenic Avian Influenza H5N1 Virus Infections in Ferrets. *PLoS ONE* **7,** e42343–21 (2012).
30. de Wit, E. *et al.* 1918 H1N1 influenza virus replicates and induces pro-inflammatory cytokine responses in extra-respiratory tissues of ferrets. *J. Infect. Dis.* (2018). doi:10.1093/infdis/jiy003
31. Fodor, E. *et al.* A Single Amino Acid Mutation in the PA Subunit of the Influenza Virus RNA Polymerase Inhibits Endonucleolytic Cleavage of Capped RNAs. *J. Virol.* **76,** 8989–9001 (2002).
32. Kashiwagi, T., Leung, B. W., Deng, T., Chen, H. & Brownlee, G. G. The N-Terminal Region of the PA Subunit of the RNA Polymerase of Influenza A/HongKong/156/97 (H5N1) Influences Promoter Binding. *PLoS ONE* **4,** e5473 (2009).
33. Tumpey, T. M. *et al.* Characterization of the reconstructed 1918 Spanish influenza pandemic virus. *Science* **310,** 77–80 (2005).
34. Vreede, F. T., Jung, T. E. & Brownlee, G. G. Model Suggesting that Replication of Influenza Virus Is Regulated by Stabilization of Replicative Intermediates. *J. Virol.* **78,** 9568–9572 (2004).
35. Fodor, E. *et al.* Rescue of influenza A virus from recombinant DNA. *J. Virol.* **73,** 9679–9682 (1999).
36. Childs, K. S., Andrejeva, J., Randall, R. E. & Goodbourn, S. Mechanism of mda-5 Inhibition by Paramyxovirus V Proteins. *J. Virol.* **83,** 1465–1473 (2009).
37. Zettl, M., Adrain, C., Strisovsky, K., Lastun, V. & Freeman, M. Rhomboid Family Pseudoproteases Use the ER Quality Control Machinery to Regulate Intercellular Signaling. *Cell* **145,** 79–91 (2011).

38. Hertzog, J. *et al.* Infection with a Brazilian isolate of Zika virus generates RIG-I stimulatory RNA and the viral NS5 protein blocks type I IFN induction and signaling. *Eur. J. Immunol.* **46,** 509 (2018).
39. Oymans, J. & Velthuis, te, A. J. W. A mechanism for prime-realignment during influenza A virus replication. *J. Virol.* **92,** e01773–17 (2018).
40. Robert, X. & Gouet, P. Deciphering key features in protein structures with the new ENDscript server. *Nucleic Acids Res* **42,** W320–4 (2014).
41. Li, H. A statistical framework for SNP calling, mutation discovery, association mapping and population genetical parameter estimation from sequencing data. *Bioinformatics* **27,** 2987–2993 (2011).
42. Dobin, A. *et al.* STAR: ultrafast universal RNA-seq aligner. *Bioinformatics* **29,** 15–21 (2012).
43. Martin, M. Cutadapt removes adapter sequences from high-throughput sequencing reads. *EMBnet.journal* **17,** 10 (2011).
44. Smith, T., Heger, A. & Sudbery, I. UMI-tools: modeling sequencing errors in Unique Molecular Identifiers to improve quantification accuracy. *Genome Research* **27,** 491–499 (2017).
45. Li, H. *et al.* The Sequence Alignment/Map format and SAMtools. *Bioinformatics* **25,** 2078–2079 (2009).
46. Leung, Y. Y. *et al.* DASHR: database of small human noncoding RNAs. *Nucleic Acids Res* **44,** D216–D222 (2016).
47. Love, M. I., Huber, W. & Anders, S. Moderated estimation of fold change and dispersion for RNA-seq data with DESeq2. *Genome Biol* **15,** 550 (2014).
48. Ignatiadis, N., Klaus, B., Zaugg, J. B. & Huber, W. Data-driven hypothesis weighting increases detection power in genome-scale multiple testing. *Nat Methods* **13,** 577–580 (2016).
49. Kim, S.-Y. & Volsky, D. J. PAGE: parametric analysis of gene set enrichment. *BMC Bioinformatics* **6,** 144 (2005).
50. Durinck, S., Spellman, P. T., Birney, E. & Huber, W. Mapping identifiers for the integration of genomic datasets with the R/Bioconductor package biomaRt. *Nature Protocols* **4,** 1184–1191 (2009).

Acknowledgements: We greatly value our discussions with R. Sun and Y. Du, who independently found that mutations in the N-terminal region of PB2, near the template exit channel of the polymerase, stimulate interferon induction[27]. We thank G.G. Brownlee, M. Freeman and F. Vreede for plasmids, J. Rehwinkel and A. Mayer for HEK 293 RIG-I -/- cells, Y. Kawaoka for the A/Brevig Mission/1/1918 (H1N1) virus, and A. Osterhaus and T. Kuiken for A/Indonesia/5/2005 (H5N1) or A/Netherlands/602/2009 (H1N1) infected ferret tissue samples. We thank Ian Sudbery for adding spliced read functionality to the umi_tools package. We thank the High-Throughput Genomics Group at the Wellcome Trust Centre for Human Genetics (funded by Wellcome Trust grant 090532/Z/09/Z) for the generation of adapter-ligated mvRNA sequencing data. This work was supported by Wellcome

Trust grant 098721/Z/12/Z, joint Wellcome Trust and Royal Society grant 206579/Z/17/Z, and a Netherlands Organization for Scientific Research (NWO) grant 825.11.029 to A.J.W.t.V; EPA Cephalosporin Junior Research Fellowship (to D.L.V.B.); support by the Intramural Research Program of NIAID, NIH, to E.d.W.; Research Grants Council of the Hong Kong Special Administrative Region, China, Project No. T11-705/14N to L.L.M.P; and Medical Research Council (MRC) programme grants MR/K000241/1 and MR/R009945/1 to E.F. and studentship to J.C.L.

Author Contributions

J.C.L., E.F., J.S. and A.J.W.t.V showed that subgenomic influenza virus RNAs stimulate IFN-β production and are bound by RIG-I. A.J.W.t.V. and J.C.L. found that mvRNAs are produced by influenza virus polymerases. D.L.V.B. designed sequencing strategies. D.L.V.B. and A.J.W.t.V. performed deep sequencing experiments and analyses. M.J.K., M.J.O.-M., H.F., and R.E.R. contributed reagents and protocols. E.d.W., D.v.R., and J.Y.S. provided ferret lung tissues. R.L.Y.F., H.Y. and L.L.M.P. performed A549 infections. A.J.W.t.V., D.L.V.B., J.C.L., and E.F. analysed data. A.J.W.t.V., J.C.L., D.L.V.B., and E.F. wrote the manuscript with input from co-authors.

Competing interests: Authors declare no competing interests.

Data availability statement: All sequencing data have been deposited in the NCBI Sequence Read Archive (SRA) under accession number SUB3758924. Gene expression data is available as Supplemental Data 1. Supplemental figures and tables are available in the Supplemental information file. Correspondence and requests for materials should be addressed to E.F. (ervin.fodor@path.ox.ac.uk) or A.J.W.t.V. (ajwt6@cam.ac.uk).

Figure 1. mvRNAs of influenza A virus are bound by RIG-I and induce IFN expression. (**a**) Models of the influenza virus ribonucleoprotein (vRNP) complex and potential activators of RIG-I. (**b**) Analysis of IFN-β promoter activity induced by the replication of segment 4, 5 or 6 vRNAs, DI RNAs or mvRNAs or by the transfection of poly(I:C). PB2, NP and tubulin expression was analysed by western blot. P-values were determined using a two-sided unpaired t-test. (**c**) IFN-β promoter activity induced by the replication of engineered, segment 5-based, short RNAs in HEK 293T cells. P-values were determined using ANOVA with multiple testing compared to the 246 mvRNA. (**d**) IFN-β promoter activity induced by the replication of engineered, segment 5-based, short RNAs in wild-type (RIG-I +/+) or HEK 293 RIG-I knockout (RIG-I -/-) cells. P-values were determined as in **c**. (**e**) Binding of segment 5-based RNAs to myc-tagged RIG-I or mouse EGF control protein (myc-ctrl). P-values were determined using ANOVA with multiple testing compared to the myc-ctrl with 246 mvRNA. All graphs show standard deviation and mean of data from three (n=3) biologically independent experiments.

Figure 2. Dysregulation of RNA replication in cells infected with WSN results in the generation of mvRNAs. (**a**) Analysis of IFN-β promoter activity (graph) and steady state vRNA and mvRNA levels (top gel) in WSN infections following overexpression of viral polymerase or viral polymerase and NP. mvRNAs were also amplified with universal primers containing adapters for sequencing (mvRNAs+adapt) and analysed by PAGE (second gel). NP, PB1 and tubulin expression was analysed by western blot. P-values were determined using ANOVA compared to lane 2. (**b**) Quantitation of mvRNAs using deep sequencing, expressed as reads per million (RPM). P-value was determined using a two-sided unpaired t-test. (**c**) mvRNA distribution per genome segment. (**d**) Size distribution of mvRNAs. (**e**) mvRNA distribution per type of intramolecular copy-choice mechanism. (**f**) Example of mvRNA formation through an intramolecular copy-choice mechanism involving a 3′ mismatch. (**g**) Model of mvRNA formation by the polymerase (model adapted from[6]). All graphs show standard deviation and mean of data from two (n=2) (**b-d**) or three (n=3) (**a,e**) biologically independent experiments.

Figure 3. The PB2 polymerase subunit of highly virulent influenza A viruses promotes mvRNA synthesis. (**a**) Analysis of mvRNA levels using primer extension (top gel) or RT-PCR (second gel) during the replication of a segment 5-based 246 nt RNA template by the WSN, BM18, NT60 and FJ02 polymerases, and IFN-β promoter activity induced by the transfection of total RNA isolated from these cells into reporter HEK 293T cells expressing luciferase. NP and PB1 expression was assessed by western blot. n=3 biologically independent experiments. P-values were determined using ANOVA with adjustments for multiple corrections compared to WSN. (**b**) Location of PB2 amino acid residues 9, 64 and 81 in the bat influenza A virus polymerase structure (PDB 4WSB). (**c**) Analysis of the effect of PB2 mutations on mvRNA formation using RT-PCR (top gel) and IFN-β promoter activity induced after transfection of total RNA isolated from these cells into luciferase reporter HEK 293T cells. PB2, NP and tubulin expression was analysed by western blot. P-values were determined using ANOVA with adjustments for multiple corrections compared to WSN. n=4 biologically independent experiments for all WSN mutants in top graph. n=3 biologically independent experiments for BM18 in top graph and all samples in bottom graph. (**d**) IFN-β promoter activity as function of PB2 mutation and mvRNA formation. Each data point was generated using the biologically independent experiments presented in **c**. P-values were determined using linear regression. All graphs show standard deviation and mean.

Figure 4. Levels of mvRNAs produced during infection correlate with innate immune responses. (**a**) Analysis of mvRNAs in A549 cells infected with WSN, VN04, VN04^{hf} using deep sequencing or PAGE. mvRNAs were amplified using universal primers containing adapters for sequencing (mvRNAs+adapt). mvRNA counts were normalised to mvRNA and mcRNA internal standards. NP vRNA and actin mRNA levels were analysed by RT-PCR. P-values were determined using ANOVA with adjustments for multiple corrections compared to the mock. (**b**) Analysis of mRNAseq of infected A549 cells showing GO terms down-regulated (left) and GO terms up-regulated (right) in VN04 infection as compared to VN04^{hf} in response to mvRNA levels. P-values were determined using a one-sample z-test (see Methods). Data are from n=4 biologically independent experiments (**a**,**b**). (**c**) Analysis of mvRNAs in lungs of ferrets one day after infection with IN05, NL09 or BM18

using deep sequencing or PAGE. NP vRNA and actin mRNA levels were analysed by RT-PCR. P-values were determined as in **a**. (**d**) Analysis of tissue mRNAseq showing GO terms enriched as function of mvRNA levels in lungs of ferrets infected with IN05, NL09 and BM18 influenza viruses. Data are from n=4 biologically independent experiments with separate mock samples for BM18, and IN05 and NL09 (**c**,**d**). One BM18 ferret was excluded from the analysis. P-values were determined as in **b**. (**e**) Model for the expression of cytokines in influenza virus infected cells. In **a** and **c** graphs show standard deviation and mean.

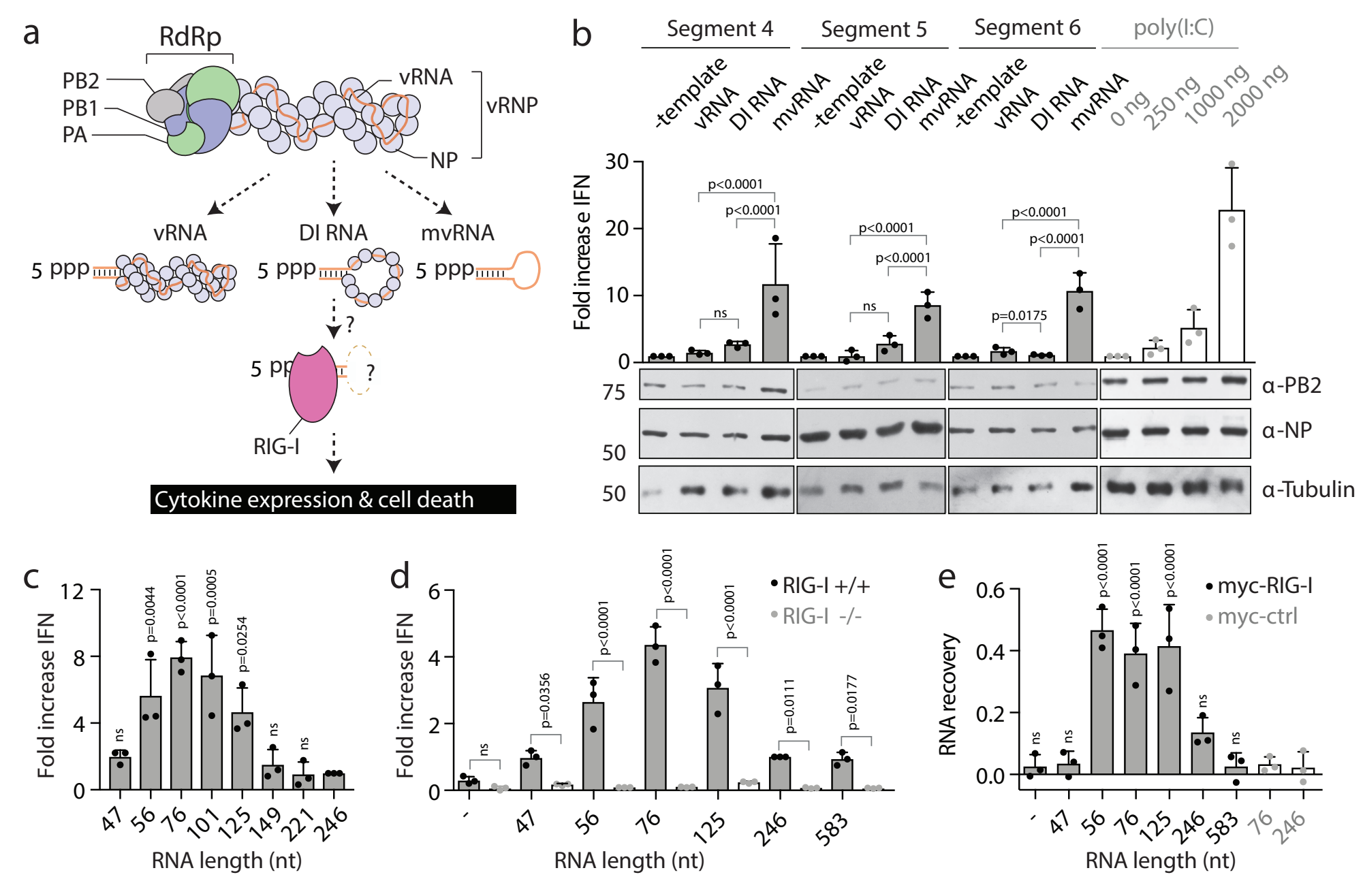
a
RdRp
PB2
PB1
PA
vRNA
vRNP
NP
vRNA
DI RNA
mvRNA
5 ppp
5 ppp
5 ppp
?
5 pp
?
RIG-I
Cytokine expression & cell death
b
Segment 4
Segment 5
Segment 6
poly(I:C)
-template
vRNA
DI RNA
mvRNA
0 ng
250 ng
1000 ng
2000 ng
Fold increase IFN
p<0.0001
ns
p=0.0175
α-PB2
α-NP
α-Tubulin
c
Fold increase IFN
p=0.0044
p<0.0001
p=0.0005
p=0.0254
RNA length (nt)
d
RIG-I +/+
RIG-I -/-
p=0.0356
p=0.0111
p=0.0177
RNA length (nt)
e
RNA recovery
myc-RIG-I
myc-ctrl
RNA length (nt)

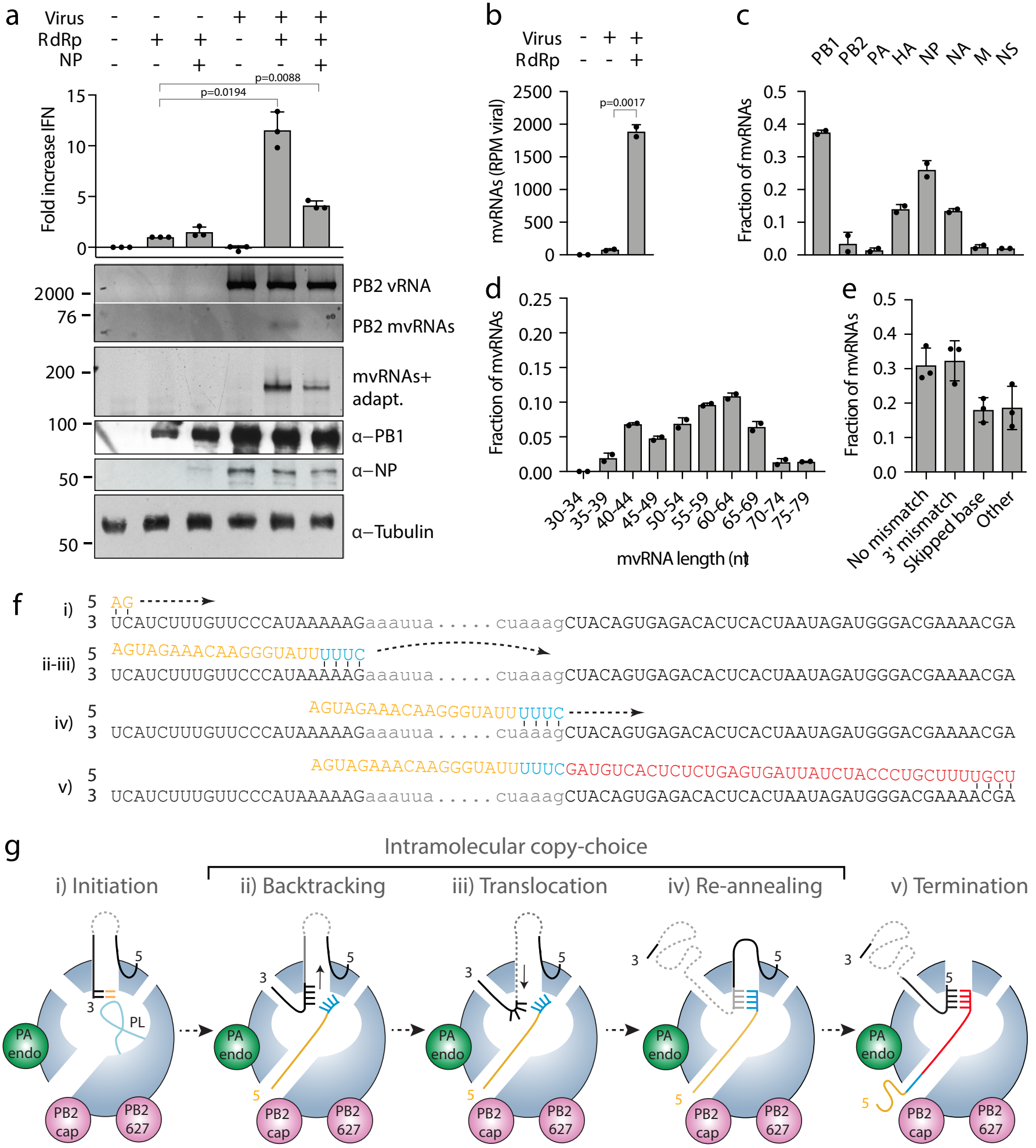
a
Virus
RdRp
NP
p=0.0088
p=0.0194
Fold increase IFN
PB2 vRNA
PB2 mvRNAs
mvRNAs+ adapt.
α–PB1
α–NP
α–Tubulin
b
mvRNAs (RPM viral)
p=0.0017
c
PB1 PB2 PA HA NP NA M NS
Fraction of mvRNAs
d
Fraction of mvRNAs
30-34 35-39 40-44 45-49 50-54 55-59 60-64 65-69 70-74 75-79
mvRNA length (nt)
e
Fraction of mvRNAs
No mismatch
3' mismatch
Skipped base
Other
f
i)
ii-iii)
iv)
v)
AG
AGUAGAAACAAGGGUAUUUUUC
AGUAGAAACAAGGGUAUUUUUCGAUGUCACUCUCUGAGUGAUUAUCUACCCUGCUUUUGCU
UCAUCUUUGUUCCCAUAAAAAGaaauua.....cuaaagCUACAGUGAGACACUCACUAAUAGAUGGGACGAAAACGA
g
Intramolecular copy-choice
i) Initiation
ii) Backtracking
iii) Translocation
iv) Re-annealing
v) Termination
PA endo
PB2 cap
PB2 627
PL

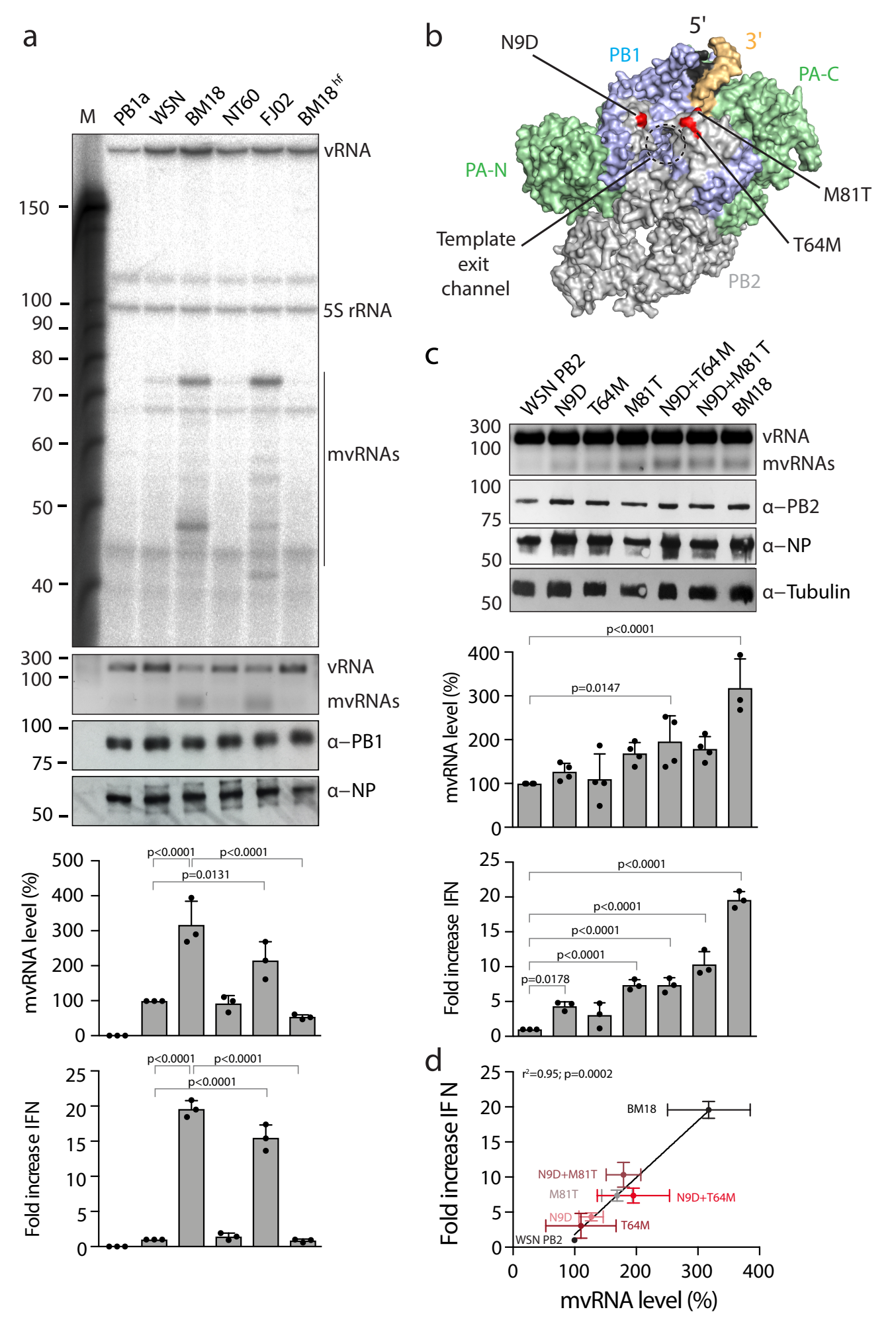
a
M
PB1a
WSN
BM18
NT60
FJ02
BM18 hf
vRNA
5S rRNA
mvRNAs
150
100
90
80
70
60
50
40
300
100
vRNA
mvRNAs
100
75
α–PB1
α–NP
50
mvRNA level (%)
p<0.0001
p<0.0001
p=0.0131
Fold increase IFN
p<0.0001
p<0.0001
p<0.0001
b
N9D
PB1
5'
3'
PA-C
PA-N
M81T
Template exit channel
T64M
PB2
c
WSN PB2
N9D
T64M
M81T
N9D+T64M
N9D+M81T
BM18
vRNA
mvRNAs
α–PB2
α–NP
α–Tubulin
mvRNA level (%)
p<0.0001
p=0.0147
Fold increase IFN
p<0.0001
p<0.0001
p<0.0001
p<0.0001
p=0.0178
d
Fold increase IF N
r²=0.95; p=0.0002
BM18
N9D+M81T
M81T
N9D+T64M
N9D
T64M
WSN PB2
mvRNA level (%)

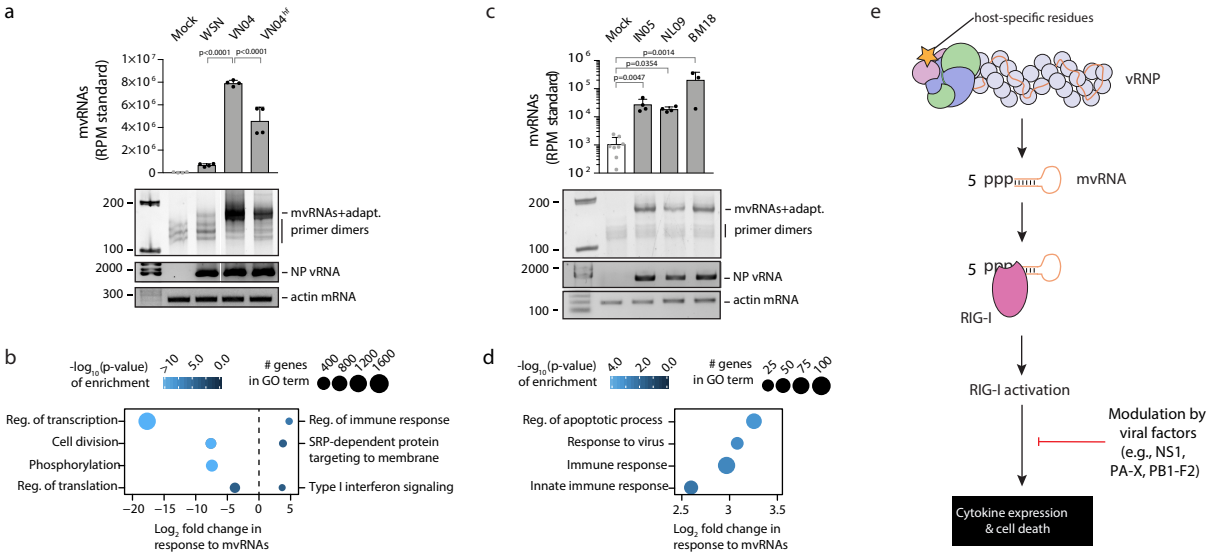
a
Mock
WSN
VN04
VN04-NF
p<0.0001
p<0.0001
mvRNAs (RPM standard)
1×10^7
8×10^6
6×10^6
4×10^6
2×10^6
0
200
100
2000
300
mvRNAs+adapt.
primer dimers
NP vRNA
actin mRNA
c
Mock
IN05
NL09
BM18
p=0.0014
p=0.0354
p=0.0047
mvRNAs (RPM standard)
10^6
10^5
10^4
10^3
10^2
200
100
2000
100
mvRNAs+adapt.
primer dimers
NP vRNA
actin mRNA
b
-log10(p-value) of enrichment
>10
5.0
0.0
genes in GO term
400
800
1200
1600
Reg. of transcription
Cell division
Phosphorylation
Reg. of translation
Reg. of immune response
SRP-dependent protein targeting to membrane
Type I interferon signaling
−20
−15
−10
−5
0
5
Log2 fold change in response to mvRNAs
d
-log10(p-value) of enrichment
4.0
2.0
0.0
genes in GO term
25
50
75
100
Reg. of apoptotic process
Response to virus
Immune response
Innate immune response
2.5
3
3.5
Log2 fold change in response to mvRNAs
e
host-specific residues
vRNP
5 ppp
mvRNA
5 ppp
RIG-I
RIG-I activation
Modulation by viral factors (e.g., NS1, PA-X, PB1-F2)
Cytokine expression & cell death

Supplementary information file

Mini viral RNAs act as innate immune agonists during influenza virus infection

Aartjan J.W. te Velthuis[1,2,*,§], Joshua C. Long[1,*], David L.V. Bauer[1,*], Rebecca L.Y. Fan[3], Hui-Ling Yen[3], Jane Sharps[1], Jurre Y. Siegers[4], Marian J. Killip[1,5], Hollie French[2], Maria José Oliva-Martín[1], Richard E. Randall[5], Emmie de Wit[6], Debby van Riel[4], Leo L.M. Poon[3], Ervin Fodor[1,§]

[1] Sir William Dunn School of Pathology, University of Oxford, South Parks Road, Oxford OX1 3RE, United Kingdom.
[2] Division of Virology, Department of Pathology, University of Cambridge, Addenbrooke's Hospital, Hills Road, Cambridge CB2 0QQ, United Kingdom.
[3] School of Public Health, University of Hong Kong, 21 Sassoon Road, Pokfulam, Hong Kong SAR, China.
[4] Department of Viroscience, Erasmus Medical Centre, 3015 CN, Rotterdam, The Netherlands.
[5] Biomedical Sciences Research Complex, University of St Andrews, North Haugh, St Andrews, Fife KY16 9ST, United Kingdom.
[6] Laboratory of Virology, Division of Intramural Research, National Institute of Allergy and Infectious Diseases, National Institutes of Health, Hamilton, Montana, USA

[*] These authors contributed equally to this work.
[§] Corresponding authors

Contents

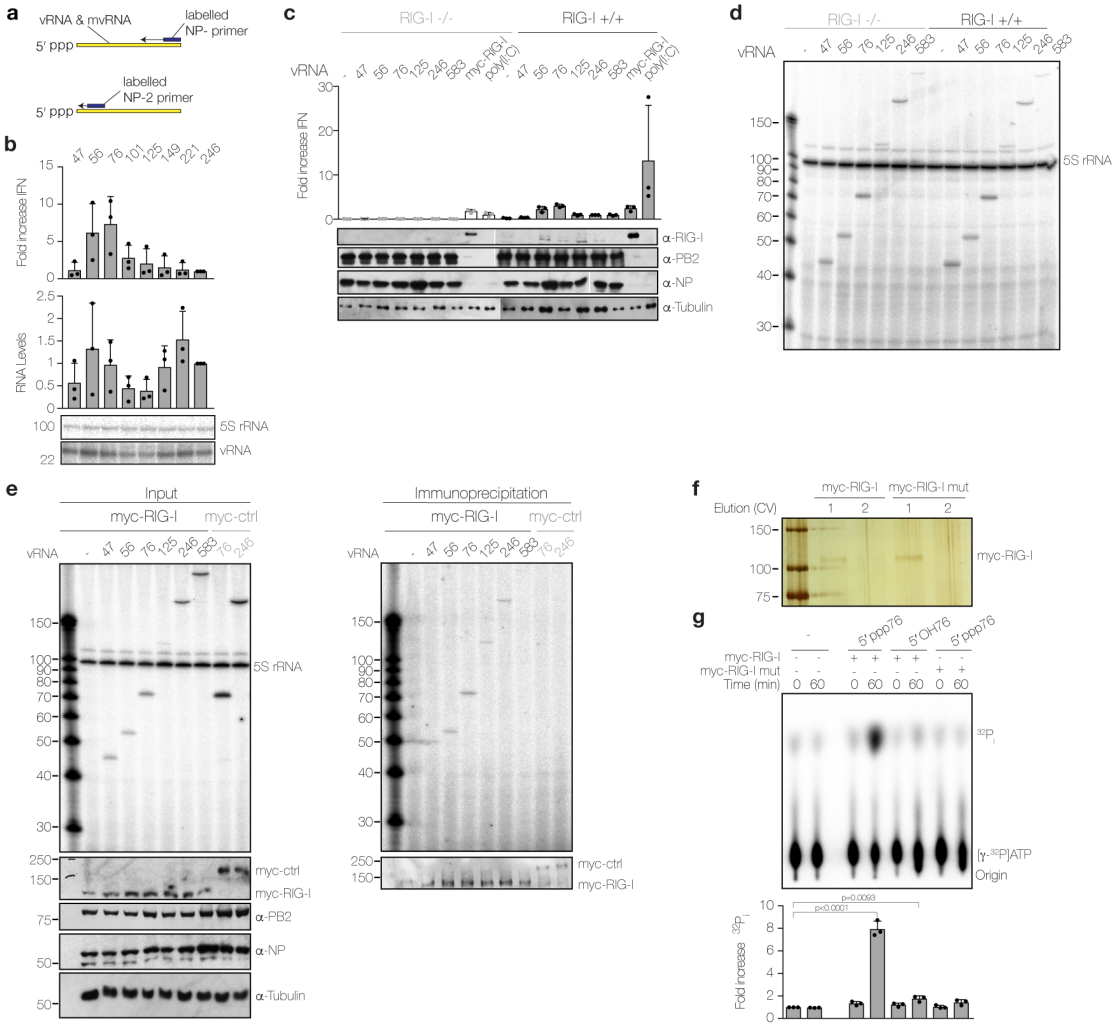

Supplementary Figure 1 I Induction of IFN-β promoter activity by replication of mvRNAs and binding of mvRNAs to RIG-I. (a) Schematic of primer extension analysis using primers binding at the 3′ end of vRNAs (NP-) or to an internal sequence (NP-2). (b) IFN-β promoter activity induced by the replication of segment 5-based vRNA templates before normalisation to RNA levels measured by primer extension with primer NP-2. Normalised data is shown in Fig. 1c. (c) INF-β promoter activity induced by the replication of segment 5-based vRNA templates in wild-type (RIG-I +/+) or RIG knockout (RIG-I -/-) HEK 293T cells expressing luciferase from an IFN-β promoter. (d) Primer extension performed with primer NP- on samples from Supplementary Fig. 1c and analysed by denaturing PAGE. Figure is a representative result of three independent experiments. (e) Detection of segment 5-derived vRNAs with the NP- primer before and after myc-RIG-I or myc-EGF immunoprecipitation. Primer extension analysis was resolved by denaturing PAGE (top panel). Protein expression was analysed by western blot (other panels). Quantified RNA levels of three independent experiments are shown in Fig. 1e. (f) SDS-PAGE and silverstain analysis of myc-RIG-I elutions per column volume (CV). Figure is representative of three independent purifications. (g) ATPase assay of wildtype myc-RIG-I or mutant (mut) in the presence of a triphosphorylated 76 nt mvRNA (5′ ppp76) or a dephosphorylated mvRNA (5′ OH76). Gel is a representative result of three independent experiments. P-values were determined using ANOVA relative to the 0 min buffer control. All graphs show standard deviation and mean of three biologically independent experiments.

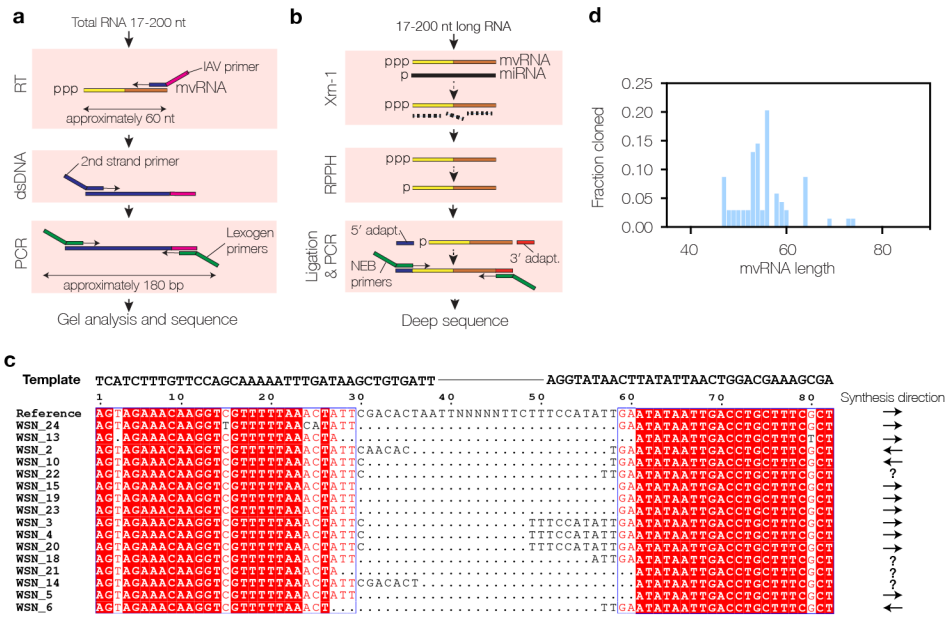

Supplementary Figure 2 | Deep sequencing schematic and alignment of cloned mvRNAs. (**a**) Schematic of deep sequencing protocol using universal primers for the influenza A virus (IAV) promoter. (**b**) Deep sequencing via adapter ligation was performed on the total small RNA fraction (RNAs 17-200 nt in length) after treatment with XRN-1 and RppH. (**c**) Alignment and (**d**) size distribution of segment 1-derived mvRNAs generated during infection with influenza A/WSN/33 (H1N1) virus in the presence of overexpressed viral polymerase. Sequences were produced after gel extraction and Sanger sequencing. The possible direction of synthesis (vRNA to mcRNA or cRNA to mvRNA) via the intramolecular copy-choice model is indicated. Unknown directions of synthesis are indicated with '?'.

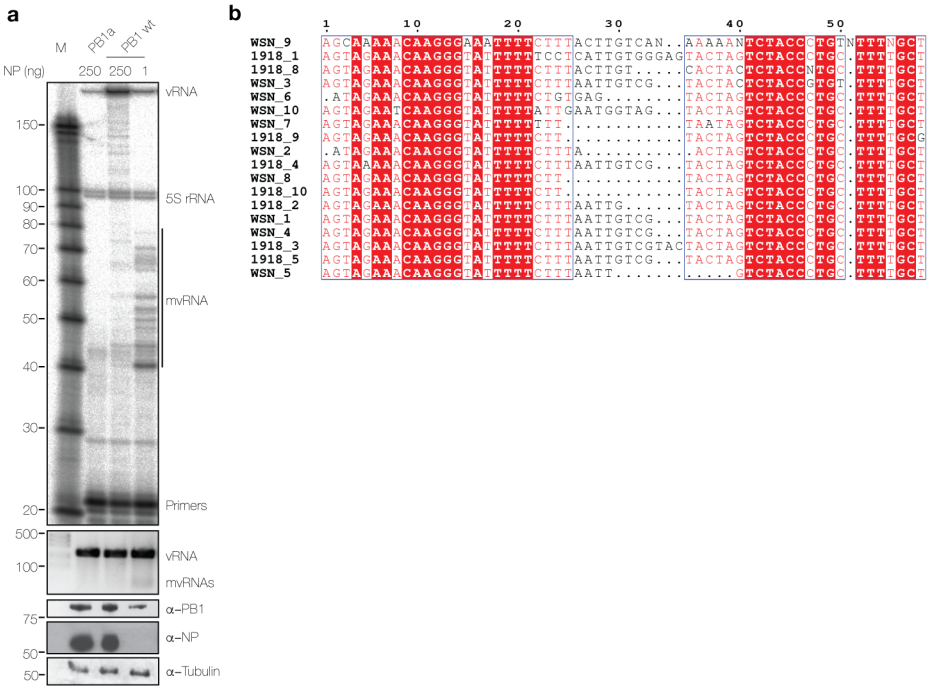

Supplementary Figure 3 | mvRNAs synthesis in replication assays with WSN polymerase in the presence of limiting NP and alignment of cloned mvRNAs. (**a**) Analysis of steady state RNA levels in replication assays with an active site mutant WSN PB1 (PB1a) or WSN PB1 wild-type (PB1 wt) and a 246-nt vRNA that was derived from segment 5 of the influenza A virus genome, in the presence of limiting NP. The NP- primer was used for primer-extension analysis of vRNA levels (top panel) and 5S rRNA was used a loading control. RT products were resolved by denaturing PAGE. vRNA and mvRNA levels were also analysed by RT-PCR and agarose gel electrophoresis (2nd panel). Viral and cellular protein levels were analysed by western blot (3rd, 4th and 5th panel). The top panel is representative of two independent experiments, while the other panels are representative of three independent experiments. (**b**) Alignment of mvRNAs generated in replication assays with the WSN and BM18 polymerases from segment 5-derived 246 nt vRNA template.

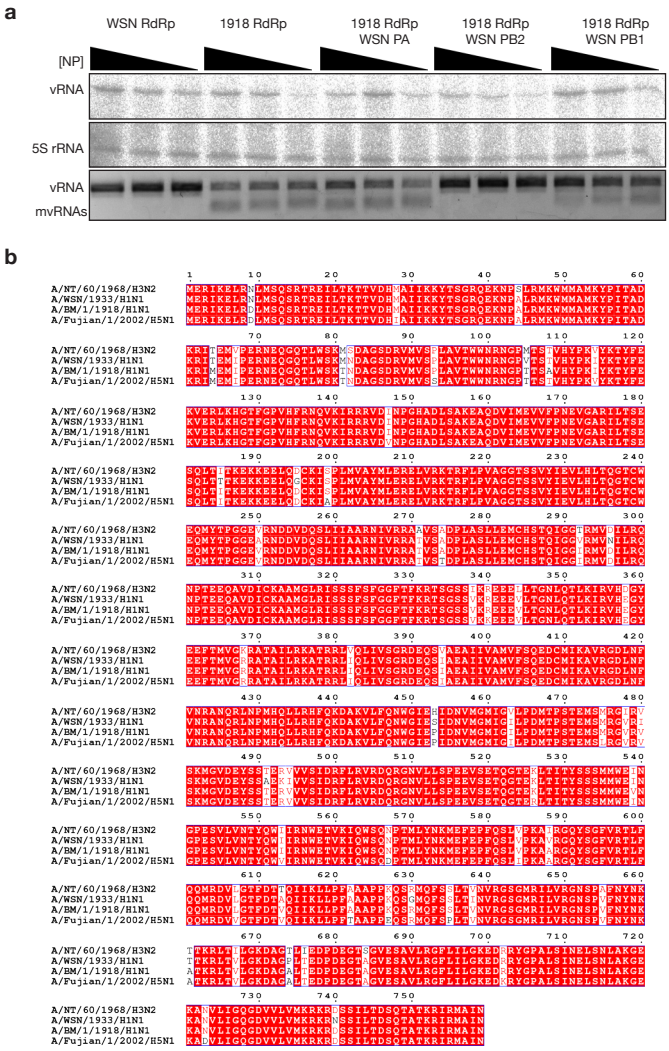

Supplementary Figure 4 | mvRNA synthesis by reassorted WSN and BM18 polymerases and sequence alignments of the PB2 subunit. (**a**) Analysis of steady state RNA levels in replication assays with WSN and BM18 polymerases and their reassortants and a 246-nt vRNA that was derived from segment 5 of the influenza A virus genome, in the presence of decreasing NP. 5S rRNA and vRNA signals were detected with radiolabeled primers and RT products were resolved by denaturing PAGE (top and middle panel). The vRNA and mvRNA signals were analysed by RT-PCR and agarose gel electrophoresis (bottom panel). The top and middle panel are representative of two independent experiments. The bottom panel is representative of four independent experiments. (**b**) Amino acid sequence alignment of the PB2 subunits of A/WSN/33 (H1N1) (accession number ACF54608), A/Brevig Mission/1/18 (H1N1) (accession number ABA55038), A/Northern Territory/60/68 (H3N2) (accession number AAA43613), and A/duck/Fujian/1/2002 (H5N1) (accession number AY585504) influenza viruses.

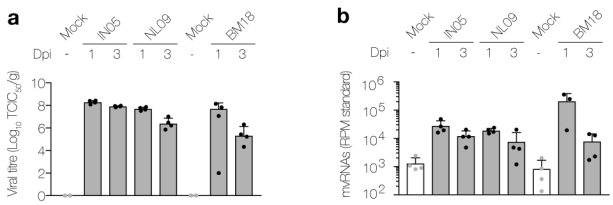

Supplementary Figure 5 | **Viral titre and mvRNA levels in ferret lungs.** (**a**) Published viral titres of ferret lung tissue samples[29,30]. (**b**) mvRNA levels in lungs of ferrets one and three days after infection with IN05, NL09 or BM18 as measured using deep sequencing. Graphs show standard deviation and mean of data from four (n=4) biologically independent animal samples. A day 1 BM18 ferret sample with low titre was excluded from the analysis.

Supplementary Table 1 | Primers for mutagenesis

Mutant	Fw/rv	Sequence (5′ to 3′)
PB1 V43I	Fw	GGAACAGGATACACCATGGATACTATTAACAGGACACATCAGTACTCAG
	Rv	CTGAGTACTGATGTGTCCTGTTAATAGTATCCATGGTGTATCCTGTTCC
PB2 E627K	Fw	CATTTGCAGCAGCCCCACCGAAGCAGAGCAGAATGCAGTTTTCTTC
	Rv	GAAGAAAACTGCATTCTGCTCTGCTTCGGTGGGGCTGCTGCAAATG
PB2 T64M	Fw	CCAATTACAGCAGACAAGAGGATAATGGAAATGATTCCTGAGAGAAATGAGC
	Rv	GCTCATTTCTCTCAGGAATCATTTCCATTATCCTCTTGTCTGCTGTAATTGG
PB2 M81T	Fw	CAGGGACAAACTTTATGGAGTAAAACGAATGACGCCGGATCAGAC
	Rv	GTCTGATCCGGCGTCATTCGTTTTACTCCATAAAGTTTGTCCCTG
Myc-RIG-I mut	Fw	AAGTTTTGAAGCAAGAGCAGCGATATTCTGTGCCCGACAGAACTGCAGC
	Rv	GAAAACTGCGCTGGCTTGGGATGTGGTCTACTCACAAAGCATTCC

Sequences of DNA primers used to generate influenza A virus polymerase subunit and RIG-I mutants. Forward (fw) and reverse (rv) primers are listed.

Supplementary Table 2 | RNA templates

Template	Sequence (5′ to 3′)
NP47	AGUAGAAACAAGGGUAUUUUUCUUUCUCGAGCGUACUAGUCUACCCUGCUUUUGCU
NP76	AGUAGAAACAAGGGUAUUUUUCUUUACUAGUGAUUUCGAUGUCACUCUGUGAGUGAUUAUCUACCCUGCUUUUGCU
NP101	AGUAGAAACAAGGGUAUUUUUCUUUAAUUGUCGUACUCACUAGUUUUGGUCGCCAUGAUUUCGAUGUCACUCUGUGAGUGAUUAUCUACCCUGCUUUUGCU
NP125	AGUAGAAACAAGGGUAUUUUUCUUUAAUUGUCGUACUCCUCUGCAUUGUCACUAGUUCGUUUGGUGCCUUUGGUCGCCAUGAUUUCGAUGUCACUCUGUGAGUACUAGUCUACCCUGCUUUUGCU
NP149	AGUAGAAACAAGGGUAUUUUUCUUUAAUUGUCGUACUCCUCUGCAUUGUCUCCGAAGAAAUAACUAGUCUGUUCGUAAGAUCGUUUGGUGCCUUUGGUCGCCAUGAUUUCGAUGUCACUCUGUGAGUGAUUAUCUACCCUGCUUUUGCU
NP246	AGUAGAAACAAGGGUAUUUUUCUUUAAUUGUCGUACUCCUCUGCAUUGUCUCCGAAGAAAUAAGAUCCUUCAUUACUCAUGUCAAAGGAGGGCACGAUCGGGCUCGUUGCCUUUUCGUCCGAGAGCUCGAAGACUCCCCGCCCCUGGAAAGACACUAGUCUCCAUCUGUUCGUAAGAUCGUUUGGUGCCUUUGGUCGCCAUGAUUUCGAUGUCACUCUGUACUAGUCUACCCUGCUUUUGCU
NP583	AGUAGAAACAAGGGUAUUUUUCUUUAAUUGUCGUACUCCUCUGCAUUGUCUCCGAAGAAAUAAGAUCCUUCAUUACUCAUGUCAAAGGAGGGCACGAUCGGGCUCGUUGCCUUUUCGUCCGAGAGCUCGAAGACUCCCCGCCCCUGGAAAGACACAUCUUCUGGUCUUGCACUUUCCAUCAGCCUUAUGAUUUCGGUUCUCAUGUCAGAUGUUCUCCCCUCUGUAUUCCCAGUGAAUGCUGCCAUAAUGGUUGGUCUGUCAAAAGGGAGAUUUCUCUGUACUGAGAACGUAGGUUGUAUGCUGAUUUGGCCCGAGGAAGCCCUCUGUUGAUUGGUGUUCCCUCCACUUCUGGUCCUUAUGGCCCAGUAUCUGCUUCUCAGUUCAAGGGUACUAGUUUAAGUUCGGUGCACAUUUGGAUGUAGAAUCGUCCAAUUCCAUCAAUCAUUUUUCCGACAGAUGCUCUGAUUUCAGUGGCAUUCUGGCGUUCUCCAUCAGUCUCCAUCUGUUCGUAAGAUCGUUUGGUGCCUUUGGUCGCCAUGAUUUCGAUGUCACUCUGUGAGUGAUUAUCUACCCUGCUUUUGCU
HA77	AGUAGAAACAAGGGUGUUUUUCCUUAUAUUUCUGAAAUCCUUCAUUUUGGUUGUUUUUAUUUUCCCCUGCUUUUGCU
HA245	AGUAGAAACAAGGGUGUUUUUCCUUAUAUUUCUGAAAUCCUAAUCUCAGAUGCAUAUUCUGCACUGCAAAGACCCAUUAGAACACAUCCAGAAACUGAUUGCCCCCAGGGAGACCAAAAGCACCAGCCUCCUCGCUGGCGCCGGCUGGGCAACAUUCCGAGGGGACCGUCCCCUCGGUAAUGGCGAAUGGGACUCUAGUACAAAAGCCUUCAUUUUGGUUGUUUUUUAUUUUCCCCUGCUUUUGCU
NA76	AGUAGAAACAAGGAGUUUUUUGAACAAACUACUUGUCAAUUUCUGGUUUGGAUUCAUUUAAACUCCUGCUUUUGCU
NA244	AGUAGAAACAAGGAGUUUUUUGAACAAACUACUUGUCAAUGGUGAACGGGAGCUCAGCACCGUCUGGCCAAGACCAAUCUACAGUAUCACCAUUCACACCACAAAAAGAAAUGAUGCUCCCACAAUCCAUAUUGAGAUUAUAUUUCCUAUUUGCAAUAUUAGGCUAAUUAUUCCGACUACCAUACAGAUCGAUCCAAUGGUUAUUAUUUUCUGGUUUGGAUUCAUUUAAACUCCUGCUUUUGCU
49-vRNA spike	AGUAGAAACAAGGGUGUUUUUUCAGAUCUCGAGUCACCCUGCUUUUGCU
37-cRNA spike	AGCAAAAGCAGGGUAGACUAGUACCCUUGUUUCUACU

Sequences of RNA templates used to perform RNP reconstitution and IFN induction assays. The NP, HA, and NA templates were expressed from plasmid DNAs containing an RNA polymerase I (Pol I) promoter. The spike RNAs were purchased as synthetic oligonucleotides.

Supplementary Table 3 | Primer-extension and RT-PCR primers

Primer name	Sequence (5′ to 3′)	Target
NP-	AGCAAAAGCAGGGTAGACTAGT	NP negative strand (3′ terminus)
NP-2	AAAGAAAAATACCCTTGTTTC	NP negative strand
5S100	TCCCAGGCGGTCTCCCATCC	5S rRNA (100 nt product)
NA-	GTTCAAAAAACTCCTTGTTTC	NA negative strand
HA-	GGAAAAACACCCTTGTTTCT	HA negative strand
NP 5'	AGTAGAAACAAGGGTATTTTTCT	NP positive strand (5′ terminus)
NP 3'	AGCAAAAGCAGGGTAGATAATC	NP positive strand (3′ terminus)
PB2v	AGCGAAAGCAGGTCAATTATAT	PB2 negative strand (3′ terminus)
PB2c	AGTAGAAACAAGGTCGTTTTTAAAC	PB2 positive strand (5′ terminus)
Lv3ga	GTTCAGACGTGTGCTCTTCCGATCTAGCG+AAAGCAGG	vRNA RT primer (contains LNA)
Lv3aa	GTTCAGACGTGTGCTCTTCCGATCTAGC+A+AAAGCAGG	vRNA RT primer (contains LNA)
Lv5	CACGACGCTCTTCCGATCTHNNNNNNNAGTAGAA+A+CAAGG	vRNA forward primer (contains LNA)
Lc3	GTTCAGACGTGTGCTCTTCCGATCTAGTAGAA+A+CAAGG	cRNA RT primer (contains LNA)
Lc5a	CACGACGCTCTTCCGATCTHNNNNNNNAGC+AAAAGCAGG	cRNA forward primer (contains LNA)
Lc5g	CACGACGCTCTTCCGATCTHNNNNNNNAGCGAAAGCAGG	cRNA forward primer
P5	AATGATACGGCGACCACCGAGATCTACACTCTTTC-CCTACACGACGCTCTTCCGATCT	vDNA and cDNA forward
i7003	CAAGCAGAAGACGGCATACGAGATACTGGTGTGA-CTGGAGTTCAGACGTGTGCTCTTCCGATCT	vDNA and cDNA reverse
Actin human fw	AGAGCTACGAGCTGCCTGAC	Actin B mRNA (forward)
Actin human rv	AGCACTGTGTTGGCGTACAG	Actin B mRNA (reverse)
Actin ferret fw	GATATTACCAGATATCTTATCAAGCTGCTGC	Actin B mRNA (forward)
Actin ferret rv	GCGGCCATCTGGGAGTGTGTAAG	Actin B mRNA (reverse)
H5N1_VN NA fw	CAATTTGGACTAGTGGGAGCAGC	NA H5N1 VN qRT-PCR (forward)
H5N1 VN NA rv	TTGAACAAACTACTTGTCAATGGTGAATG	NA H5N1 VN qRT-PCR (reverse)
NA rv	GCAACTCAGCACCGTCTGGCC	NA qRT-PCR (reverse)
NA 1918 fw	TGCTTCTGGGTTGAATTAATCAGGG	NA BM 1918 qRT-PCR (forward)
NA NL fw	GCTTCTGGGTTGAACTAATCAGAGGG	NA NL 2009 qRT-PCR (forward)
NA IND fw	GTTTCTGGGTTGAGTTGATCAGAGGG	NA Ind H5N1

Sequences of DNA primers used to perform primer extension reactions and RT-PCR reactions. Targets of the primers are listed. Some RT primers contain LNA bases. The location of these LNA bases in the primers is indicated with +N, where N represents the base.

Raw images Figure 1

Figure 1b

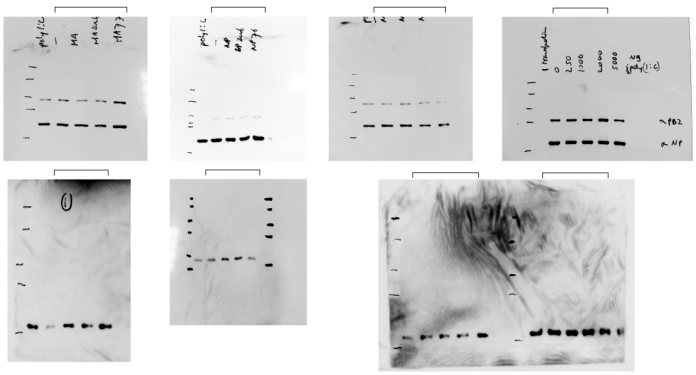

Raw images Figure 2

Figure 2a

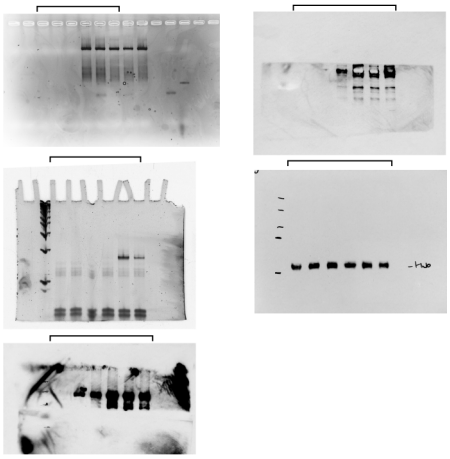

Raw images Figure 3

Figure 3a

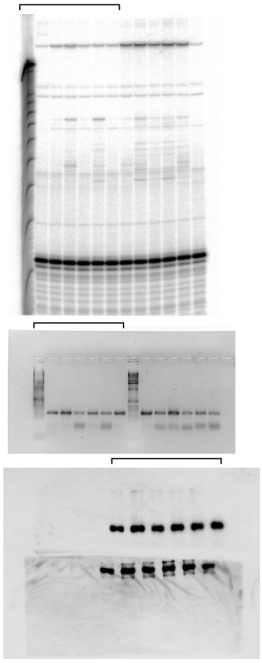

Figure 3c

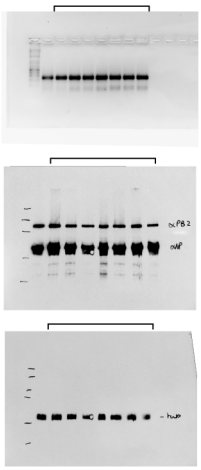

Raw images Figure 4

Figure 4a

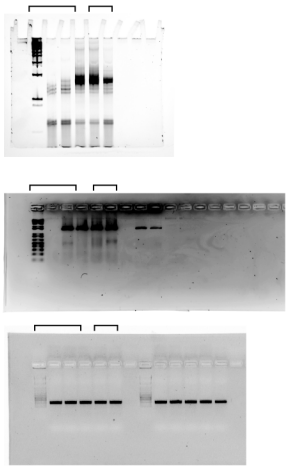

Figure 4c

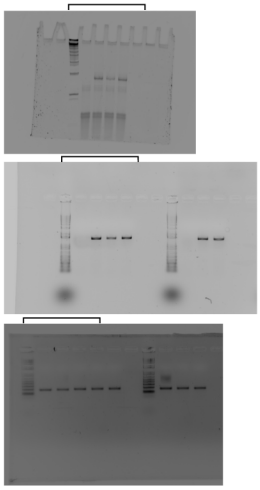

Raw images Supplementary Figure 1

Figure S1b

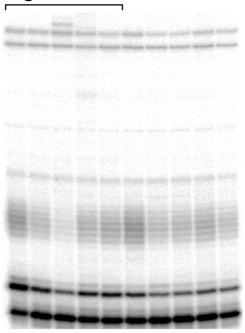

Figure S1c

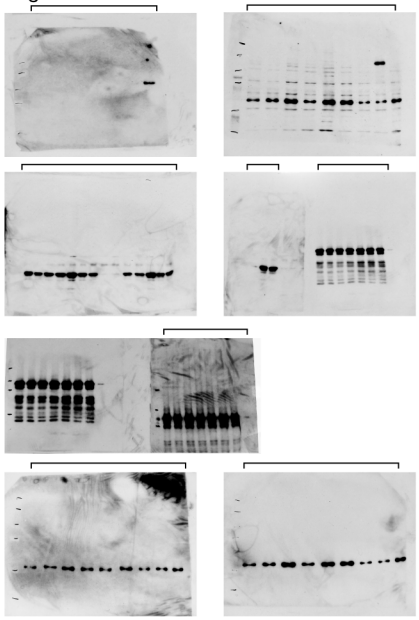

Figure S1d

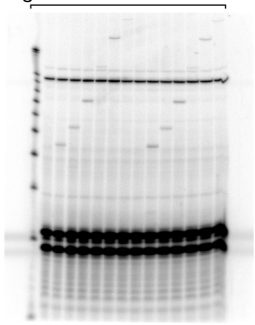

Figure S1e

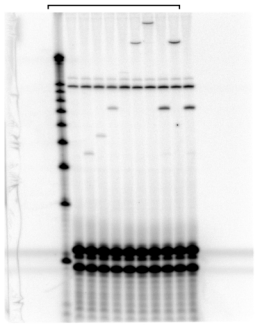

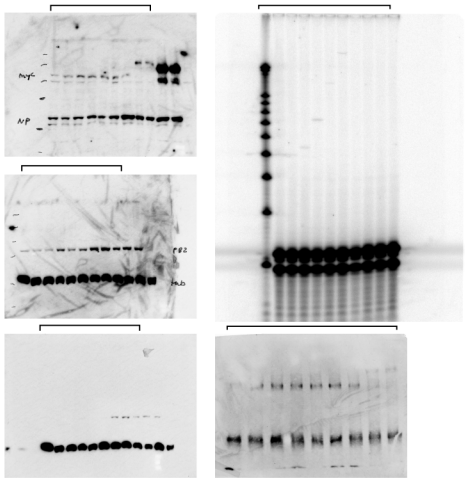

Figure S1f

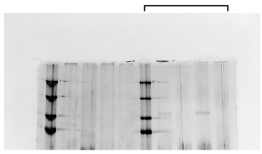

Figure S1g

Raw images Supplementary Figure 3

Figure S3a

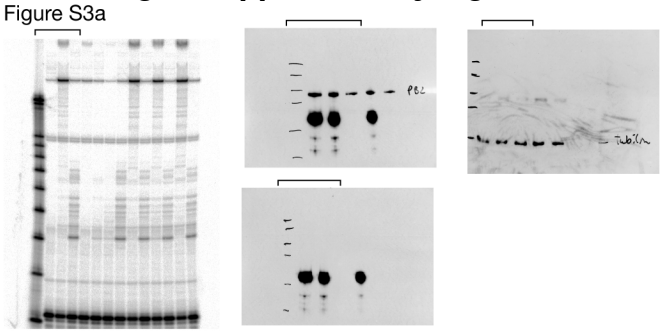

Raw images Supplementary Figure 4

Figure S4